Transportation Research Part E 192 (2024) 103757

Contents lists available at ScienceDirect

Transportation Research Part E

journal homepage: www.elsevier.com/locate/tre

# Constructing a routable multimodal, multi-cost, time-dependent network model with all emerging mobility options: Methodology and case studies

Lindsay K. Graff [a], Katherine A. Flanigan [a,*], Sean Qian [b]

[a] Department of Civil and Environmental Engineering, Carnegie Mellon University, Pittsburgh, PA 15213, United States of America
[b] Department of Civil and Environmental Engineering, Heinz College of Information Systems and Public Policy, Carnegie Mellon University, Pittsburgh, PA 15213, United States of America

ARTICLE INFO

Dataset link: https://github.com/lgraff/nomad

*Keywords:*
Multimodal
Network modeling
Accessibility
Shared mobility
Generalized travel cost
Micromobility

ABSTRACT

Cities aiming to improve their transportation networks are integrating emerging mobility options at a rapid pace. These modes provide commuters with greater flexibility to construct more convenient trips and reach a larger set of essential service destinations. A few open-source tools allow planners to conduct multimodal routing analysis in time-dependent networks, but they do not sufficiently capture the full set of travel mode combinations and disutility factors perceived by individual travelers. To this end, we introduce NOMAD: Network Optimization for Multimodal Accessibility Decision-making. NOMAD integrates the personal vehicle, transportation network company, carshare, public transit, personal bike, bikeshare, scooter, walking, and feeder micro-transit modes into a unified routable network model. A generalized travel cost function incorporates the following disutility factors: monetary cost, day-to-day mean travel time, (un)reliability as represented by day-to-day 95th percentile travel time, crash risk, and physical discomfort. The proposed open-source tool can be used to create multimodal travel cost matrices, which may immediately serve as an input for accessibility analysis and other policy decisions related to emerging mobility options. This paper develops the network model that forms the basis of NOMAD and demonstrates four use cases in Pittsburgh, PA.

## 1. Introduction

As the mobility landscape evolves, several cities have developed plans to make their multimodal transportation networks more efficient, affordable, reliable, safe, and equitable, all with the goal of improving access to goods and services (City of Austin, 2022; City of Boston, 2017; City Of Pittsburgh, 2022). In these cities and others, travelers are no longer limited to a personal vehicle or fixed-route public transit. Rather, they may use emerging shared mobility services, which include transportation network companies (TNCs), bikeshare, carshare, shared scooters, and micro-transit, to construct convenient multimodal routes from end to end. These shared mobility modes enable travelers to reach a larger set of destinations by removing the financial cost of vehicle parking and the constraints associated with schedule-based, fixed-route transit. Though travelers have many options, their decision to take one mode versus another reflects their sensitivity to a variety of cost factors (Quarmby, 1967; Bhat, 2000; Susilo and Cats, 2014). For example, public transit is cheap but potentially unreliable and difficult to reach, whereas TNC is an expensive but usually faster option. Moreover, route selection is dependent on departure time due to the transit schedule and fluctuations in traffic flow.

* Corresponding author.
*E-mail addresses:* lgraff@andrew.cmu.edu (L.K. Graff), kflaniga@andrew.cmu.edu (K.A. Flanigan), seanqian@cmu.edu (S. Qian).

https://doi.org/10.1016/j.tre.2024.103757
Received 3 May 2024; Received in revised form 1 August 2024; Accepted 1 September 2024
Available online 25 September 2024

The proliferation of shared modes has led to developments in research relating to multimodal routing analysis, which involves identifying the optimal route between origin–destination (O-D) pairs. Routing analysis is important because it is a requisite step to evaluating accessibility in a transportation network and quantifying the potential impact of future network investments (Levinson and King, 2020). While early research focused on O-D routing strictly in the personal vehicle and/or public transit networks, more recent literature incorporates shared mobility modes (Pereira et al., 2024a; Qian and Niemeier, 2019; Liu and Miller, 2022; Liezenga et al., 2024). Previous research also solved for the optimal path solely with respect to travel time, whereas newer literature aims to capture the effect of additional travel disutility factors such as monetary cost and time variability (El-Geneidy et al., 2016b; Arbex and Cunha, 2020). Still, researchers have yet to introduce a routable unified network model that includes all emerging mobility services and relevant travel cost factors.

A few popular open-source tools, namely OpenTripPlanner (OpenTripPlanner, 2024a) and R5 (Pereira et al., 2021), allow planners to conduct multimodal routing analysis in time-dependent networks. However, we contend that these tools do not reflect the full set of mobility options available to travelers (e.g., trips that sequentially use bikeshare and TNC, or those involving both feeder micro-transit and main fixed-route transit). Nor do they account for the array of costs that individual travelers perceive depending on their costs sensitivities. To this end, we introduce NOMAD: Network Optimization for Multimodal Accessibility Decision-making.[1] NOMAD integrates a complete set of mobility options and diverse travel costs into a routable time-dependent network model. The full set of travel modes includes personal vehicle, transportation network company, carshare, public transit, personal bike, bikeshare, scooter, walking, and feeder micro-transit. Our model allows for all practical combinations of these modes. A single generalized cost function accounts for the following disutility factors: monetary cost, day-to-day mean travel time, (un)reliability as represented by day-to-day 95th percentile travel time, crash risk, and physical discomfort. The model accounts for individual travelers who have different sensitivities to each of the five cost attributes. This paper designs the multimodal network model that forms the basis of NOMAD, whereas the optimization of multimodal networks is beyond the scope of this paper and discussed in future work.

Our proposed model can be used to create multimodal travel cost matrices, which may immediately serve as an input for downstream accessibility analysis. Policymakers can also use it to evaluate changes in system-level accessibility based on adjustments in prices, network infrastructure, and mobility service areas and schedules. This information can ultimately inform the network optimization of mobility services and infrastructure given accessibility objectives and budget constraints, allowing transportation planners to make decisions on future investments. Applications can further be developed for community stakeholders involved with Mobility as a Service (MaaS). These include estimating the pattern of network usage for each mode and facility, which entails aggregating least-cost paths for all individuals across multiple O-D pairs.

The remainder of this paper is structured as follows. Section 2 provides an overview of accessibility analysis, open-source routing engines, and routing algorithms, all from a multimodal, multi-cost, and time-dependent perspective. This section also highlights the research gaps and opportunities addressed by our work. Section 3 presents the design of NOMAD, including the topology of the multimodal network model, the generalized travel cost function, and the process for measuring the generalized travel cost of any O-D pair. In Section 4, we demonstrate four use cases of the model on a subset of the transportation network in Pittsburgh, PA. Section 5 highlights conclusions and identifies opportunities for future work.

## 2. Literature review

This topic spans three related areas of literature: (1) accessibility analysis, (2) multimodal routing engines, and (3) multimodal route-finding algorithms and network models.

### *2.1. Accessibility analysis*

Accessibility has been quantified in different ways over decades of research. Table 1 categorizes the accessibility literature along four dimensions that are discussed below. In terms of calculating accessiblity, spatial metrics on the O-D level simply report the travel cost between a given O-D pair (Curtis and Scheurer, 2010), where the travel cost is associated with the theoretically optimal path. Origin-based cumulative opportunities metrics count the number of opportunities within some travel cost contour relative to an origin. An "opportunity" in this context indicates a point of interest, such as a place of employment, school, or hospital. Origin-based gravity metrics are similar, though each opportunity is discounted by some function of its travel cost with respect to the origin (Curtis and Scheurer, 2010; Geurs and van Wee, 2004). From a different perspective, destination-based metrics proposed in Mavoa et al. (2012) and Gehrke et al. (2020) quantify the number of origins that can reach a given destination within some travel cost threshold.

As cities introduce newer transportation modes, researchers have begun to evaluate accessibility in networks that enable multimodal trips with a variety of shared modes and micromobility. Abdelwahab et al. (2021) compare accessibility to jobs based on four possible mode combinations: personal vehicle, transportation network company (TNC), public transit/walking, and public transit/TNC. They define a generalized travel cost that is the sum of monetary cost and travel time weighted by a traveler's value of time (average wage, in their paper). They conclude that integrating public transit with TNC does not noticeably increase job access, indicating that TNC is likely too expensive as a first mile solution. Pereira et al. (2024a) present a similar finding upon investigating the effect of TNC as a first-mile leg to public transit. Djurhuus et al. (2016) measure accessibility as the sum of area reachable by

[1] The implementation of NOMAD with experiments is available at the following link: https://github.com/lgraff/nomad.

**Table 1**
Literature review: accessibility evaluation.

| Study | Travel modes | Travel costs | Conducts time-dependent analysis | Level(s) of population analysis |
|---|---|---|---|---|
| Owen and Levinson (2015) | Personal vehicle, PT, walk | Travel time | Yes (minute-level) | Census block group |
| Djurhuus et al. (2016) | PT, personal bike, walk | Travel time | No | City vs. suburbs vs. rural area |
| El-Geneidy et al. (2016a) | PT, walk | Travel time | Yes (hour-level) | Census tract, social decile group |
| El-Geneidy et al. (2016b) | PT, walk | Travel time, monetary cost | No | Census tract |
| Chen et al. (2017) | PT, walk | Travel time | No | Grid cell |
| Conway et al. (2017) | PT, walk | Travel time, (un)reliability | Yes (minute-level) | Grid cell |
| Farber and Fu (2017) | PT, walk | Travel time | Yes (minute-level) | TAZ |
| Guzman et al. (2017) | Personal vehicle, PT | Travel time, monetary cost | No | Income group |
| Pritchard et al. (2019) | Personal vehicle, PT, personal bike, walk | Travel time | Yes (hour-level) | TAZ |
| Tahmasbi et al. (2019) | Personal vehicle, PT, walk | Travel time | No | TAZ, income group |
| Arbex and Cunha (2020) | PT, walk | Travel time, (un)reliability, discomfort | No | Grid cell |
| Gehrke et al. (2020) | Personal bike | Travel time, elevation, level of traffic stress | No | Census block, cyclist type |
| Abdelwahab et al. (2021) | Personal vehicle, PT, TNC, walk | Travel time, monetary cost | No | TAZ |
| Liu and Miller (2022) | PT, scooter, walk | Travel time, monetary cost | No | Grid cell |
| Saraiva and Barros (2022) | Personal vehicle, PT, personal bike, walk | Travel time | Yes (minute-level) | Individual, socio-economic class |
| Braga et al. (2023) | PT, walk | Travel time, (un)reliability | Yes (minute-level) | Grid cell, income group |
| Pereira et al. (2024a) | PT, TNC, walk | Travel time, monetary cost | Yes (minute-level) | Grid cell, income group |
| This paper | Personal vehicle, TNC, carshare, PT, personal bike, bikeshare, scooter, walking, feeder micro-transit | Travel time, monetary cost, (un)reliability, risk, discomfort | Yes (minute-level) | Generic socio-demographic population group |

*Notes*: "PT" = fixed-route public transit; "TAZ" = traffic analysis zone.

a combination of public transit/personal bike/walking within a travel time threshold. As expected, they find that total accessible area increases when travelers can use a bike for the first segment since more transit stops can be reached. Similarly, Pritchard et al. (2019) quantify job accessibility and account for multimodal trips consisting of public transit/personal bike/walking. Their results show that bike usage as a first mile solution increases job access in certain parts of the city that already have better transit service, while other areas do not experience the same benefit. Extending beyond biking, Liu and Miller (2022) assess the potential upside of dockless scooters as a first/last-mile leg to public transit.

Recent studies have expanded accessibility analysis for transportation planning by considering disutility factors beyond travel time. One common extension is the inclusion of monetary cost. For example, El-Geneidy et al. (2016b) combine travel time and transit fare cost to calculate the generalized travel cost between O-D pairs, expressing the final cost both in terms of travel time and money. Guzman et al. (2017) adopt a similar method to compare accessibility by personal vehicle and public transport. Other studies, including Abdelwahab et al. (2021) and Pereira et al. (2024a), examine the impact of monetary cost on accessibility in the context of TNCs as a complement to transit. Similar to El-Geneidy et al. (2016b), Abdelwahab et al. (2021) calculate the minimum generalized travel cost between an O-D pair and use this cost as an input to their accessibility metric. Pereira et al. (2024a) take a different approach by identifying all Pareto-optimal paths with respect to monetary cost and travel time, counting a destination as reachable if at least one Pareto path satisfies both a monetary cost budget and travel time threshold constraint. Their method is derived from previous work by Conway and Stewart (2019) that proposes a way to construct the Pareto frontier of paths characterized by two travel costs.

Other studies account for the effect of additional travel disutility factors. In quantifying the accessibility impacts of new bike infrastructure, Gehrke et al. (2020) adjust path travel time by elevation gain and road preference. The authors identify the optimal path between each O-D pair and then measure the percentage of each path that uses roads classified with low levels of traffic stress. Their results show that cyclist access to jobs generally declines when travel time and low-stress conditions must be jointly met. Arbex and Cunha (2020) analyze the effect of travel time variability and crowding discomfort on transit accessibility by constructing a generalized cost that includes a travel time buffer and passenger density value. Two related studies by Liu et al. (2023) and Braga et al. (2023) highlight the importance of accounting for some measure of transit reliability. Rather than inferring the travel time between an O-D pair from published transit schedules, both studies use historical data and conclude that schedule-based-accessibility is often an overestimation. More extensively, Cui and Levinson (2018) define a "full cost accessibility" framework that integrates travel time, crash risk, emissions, and monetary cost into a single generalized travel cost function, though they do not demonstrate their method on a real network.

Frequently in the transportation literature, accessibility metrics calculated at one departure time are used to represent daily accessibility. The limitation with this approach is that intraday variations in traffic congestion and transit schedules can have significant impacts on the travel time between an O-D pair (Anderson et al., 2013; Moya-Gómez and García-Palomares, 2017). Some studies account for these fluctuations by calculating accessibility at a higher temporal resolution (Owen and Levinson, 2015; Farber and Fu, 2017; Pritchard et al., 2019; Stępniak et al., 2019; Braga et al., 2023). In particular, Owen and Levinson (2015) report accessibility metrics on the minute-level to show how low-frequency transit can leave some regions underserved for sustained periods of time. Conway et al. (2017) calculate the O-D travel time matrix for each departure time at every minute within a departure time window, aggregating the values for each O-D pair by choosing the median travel time within the window. Braga et al. (2023) employ this method to compare median travel time according to the schedule with median travel time according to historical performance. Furthermore, Stępniak et al. (2019) provide insight into the appropriate level of temporal resolution by comparing metrics aggregated at different time scales. For a full literature review of accessibility studies that include a temporal dimension, see Stępniak et al. (2019).

Moreover, several studies have focused on developing equity measures that identify gaps in accessibility across geographic regions. Many of these studies compare metrics across areas that are characterized by different incomes (Foth et al., 2013; El-Geneidy et al., 2016a; Kelobonye et al., 2019; Tahmasbi et al., 2019; Guzman et al., 2017). This method is useful for making generalizations about the relationship between socioeconomic conditions and access to services. However, it assumes a homogeneous population living in each geographic area and neglects the influence of demographic characteristics such as age, disability status, and household composition that have been shown to influence travel patterns (Susilo and Cats, 2014). Recent literature draws attention to the importance of considering individual traveler preferences. Kar et al. (2023) propose the concept of "inclusive accessibility" and measure accessibility for forty surveyed travelers who differ in their perceptions of walking disutility. Saraiva and Barros (2022) also adopt an individual approach, developing per-person metrics which are subsequently aggregated by economic class.

### 2.2. Multimodal routing engines

Calculating accessibility metrics requires an O-D travel cost matrix that stores the travel cost for all selected O-D pairs. Several open-source software packages provide routing optimization engines to accomplish this task, and Alessandretti et al. (2023) enumerate the tools available. Here, we detail four routing engines that are most relevant for our research: GraphHopper, Valhalla, OpenTripPlanner, and R5. The GraphHopper library (GraphHopper, 2024) provides single-mode routing optimization for a variety of modes, including public transit, private vehicle, personal bike, personal scooter, walking, and commercial truck. Each network edge is weighted by a generalized travel cost that is a linear sum of the edge's distance and travel time, and users can adjust the influence that elevation and road type have on the calculation of edge travel time. The Valhalla routing engine (Valhalla, 2024) appears similar in design to Graphhopper. It offers single-mode routing optimization for a wide set of modes, though a multimodal routing engine limited to transit/walking is currently in beta version. For single-mode travel, the network edge cost is some function of travel time. Users can also penalize the edge cost based on elevation and road type, among other factors.

OpenTripPlanner (2024a) is perhaps the most complete in terms of modes offered. Under certain conditions, it can identify optimal multimodal routes that include public transit, private vehicle, personal bike, bikeshare, shared scooters, carshare, and walking. We note that bikeshare, scooters, and carshare are only included if the operators provide data for these modes in the form of the General Bikeshare Feed Specification (GBFS). The ability to include Uber TNC vehicles is currently a sandbox feature under development, and micro-transit is not considered. OpenTripPlanner returns routes that are optimized by generalized travel cost, though the precise form of this function is unclear. The function appears to be capable of considering travel time, road safety for bikers and pedestrians, number of transfers, and elevation, where users can configure specific parameters to adjust the sensitivity of each travel cost factor.

More recently, Pereira et al. (2021) introduced r5r and r5py, multimodal routing packages implemented in R and Python, respectively, based on the R5 engine (Conveyal, 2024b). Street segments are characterized by a travel time and monetary cost, and the biking and walking travel times are adjusted depending on elevation gain. The routing engine also considers a road's level of traffic stress, avoiding roads for bikers that exceed a user-defined maximum stress value. To calculate the O-D travel cost matrix, R5 uses an extended version of the RAPTOR algorithm (Delling et al., 2015), which returns Pareto-optimal routes based on both monetary cost and travel time. Users can input the maximum monetary cost they are willing to pay such that the route used to calculate travel time between an O-D is the fastest one that does not exceed the maximum monetary cost. Furthermore, R5 captures travel time variation within a departure window by calculating the shortest path for all departure times within the window on the minute-level and then reporting the median (or other percentile) result.

**Table 2**
Literature review: multimodal route-finding algorithms and network models.

| Study | Use case | Travel modes | Algorithm(s) |
|---|---|---|---|
| Delling et al. (2009) | RTRP | Personal vehicle, PT, flight, walk | Label-Constrained Dijkstra |
| Zhang et al. (2011) | RTRP | Personal vehicle, PT, personal bike, walk | Dijkstra |
| Delling et al. (2013) | RTRP | Personal vehicle, taxi, PT, personal bike, bikeshare, walk | Multi-Label Correcting; Multimodal Multicriteria Round-Based Public transit Optimized Router |
| Hrnčíř and Jakob (2013) | RTRP | Personal vehicle, TNC, PT, personal bike, bikeshare, walk | Dijkstra, A* |
| Dibbelt et al. (2015) | RTRP | Personal vehicle, PT, flight, walk | Label-Constrained; Dijsktra |
| Huang et al. (2019) | RTRP | PT, carpool | Dijkstra |
| This paper | Routing analysis | Personal vehicle, TNC, carshare, PT, personal bike, bikeshare, scooter, walking, feeder micro-transit | Decreasing Order of Time[a] |

*Notes*: "RTRP" = real time route planning; "PT" = public transit.
[a] Algorithm proposed in Chabini (1998).

### 2.3. Multimodal route-finding algorithms and network models

Central to the proposed methodology is the task of finding the shortest, or least cost, path in a multimodal network. This paper uses elements of the literature of Table 2 to design a routable multimodal network model. In doing so, this work bridges the aforementioned literature on accessibility analysis with the body of research related to multimodal route-finding in large-scale networks. Much of the previous multimodal route-finding research summarized in Table 2 is focused on the process of efficiently finding optimal paths with respect to the commonly used criteria of travel time and number of transfers. This process-driven research, which mostly centers on improving algorithmic efficiency, is necessary for the development of mobile applications such as Moovit and Citymapper that people use for real-time navigation in an increasingly multimodal world (Dimokas et al., 2018). Unlike this type of routing research, this paper does not concentrate on the algorithmic or runtime efficiency components of pathfinding, nor does it outline a procedure for finding a multimodal route for many users in real-time. Instead, the research objective is to develop a tool that can determine optimal paths for individual travelers when multiple modes are available.

### 2.4. Identified research gaps and opportunities

Reviewing the accessibility literature reveals many independent attempts to consider multiple travel modes, several travel costs, time-dependency, and individual traveler groups. However, we did not identify research that simultaneously considers all four elements. Integrating them is non-trivial, as it requires specific network design regarding edges, nodes, and their respective impedances.

OpenTripPlanner and R5, which enable routing analysis and provide the O-D travel cost matrices that are pivotal to accessibility calculations, are certainly well-developed in terms of their multimodal and multi-cost capabilities. Still, neither one captures an exhaustive set of travel mode combinations and the full array of costs. OpenTripPlanner includes bikeshare, scooter, and carshare only if a GBFS real-time data feed is provided, which neglects cases where these modes exist but the regional operators choose not to publish real-time location data. Uber can only be added in a sandbox testing environment, and micro-transit is not an option. Thus, it is not possible to model all trips. One example is a trip that sequentially uses bikeshare and TNC in a city that does not publish GBFS micromobility data. We also cannot conclusively determine how the generalized travel cost is defined. For example, it appears that some measure of bike safety is incorporated but the metric itself is unclear.

Upon testing the r5r package interface to the R5 routing engine and examining its source code (Pereira et al., 2024b), we found that users are required to choose either walking or personal bike as access and egress modes when planning routes with public transit. An error message indicates that park-and-ride and bikeshare options are currently not supported. Moreover, TNC, carshare, scooter, and micro-transit are not included as travel modes. This hinders its ability to model feasible trips, such as those that sequentially use transit and scooter. The r5r package can return Pareto-optimal paths based on travel time and monetary cost, yet its ability to account for other factors is more limited. Though it considers safety risk by preventing travel along road segments whose level of traffic stress exceeds a user-defined value, we contend that risk should be defined in a more granular way. Level of traffic stress is a five-category metric derived from many safety-related factors. Those factors may instead be used directly to define safety for each road and intersection at the discretion of users. We also observe that r5r does not account for retrospective travel times, an important consideration for transit riders who make decisions based on historical reliability. In addition, a detailed description of the network modeling methodology is missing from both packages. The r5r implementation is associated with a short paper that explains a few of its available functions and use cases (Pereira et al., 2021), while additional information is spread across disparate sources such as released tutorials, package documentation (Pereira et al., 2024c) and Conveyal's online manual (Conveyal, 2024a). The case is similar for OpenTripPlanner, whose functionality is described both on its Github page (OpenTripPlanner, 2024b) and online documentation manual (OpenTripPlanner, 2024a).

To address these gaps, we introduce an expansive open-source routing tool named NOMAD: Network Optimization for Multimodal Accessibility Decision-making. NOMAD can identify optimal paths in a multimodal, time-dependent network subject to generalized travel costs for individual traveler groups. In particular, it accounts for the following elements:

**Table 3**
List of notation.

| | |
|---|---|
| $\mathcal{M}$ | Set of modes, with the exception of the walking and feeder micro-transit modes, included in the multimodal network |
| $G_m$ | Graph associated with travel mode $m \in \mathcal{M}$ |
| $N_m$ | Set of graph nodes associated with $G_m$ |
| $A_m$ | Set of graph edges associated with $G_m$ |
| $N_{dr}$ | Set of street intersection nodes in the drivable network |
| $A_{dr}$ | Set of street segment edges in the drivable network |
| $N_{pk}$ | Set of parking nodes |
| $A_{pk,cnx}$ | Set of edges that connect parking nodes to their nearest street intersection node in the drivable network |
| $N_b$ | Set of street intersection nodes in the bikeable network |
| $A_b$ | Set of street segment edges in the bikeable network |
| $N_{css}$ | Set of carshare station nodes |
| $A_{css,cnx}$ | Set of edges that connect carshare station nodes to their nearest street intersection node in the drivable network |
| $N_{ps}$ | Set of fixed-route transit physical stop nodes |
| $N_{rt}$ | Set of fixed-route transit virtual route nodes |
| $A_{rt}$ | Set of fixed-route transit route edges |
| $A_{board}$ | Set of edges from physical stop nodes to associated virtual route nodes (representing the process of waiting and boarding) |
| $A_{alight}$ | Set of edges from virtual route nodes to associated physical stop nodes (representing the process of alighting) |
| $N_{bss}$ | Set of bikeshare station nodes |
| $A_{bss,cnx}$ | Set of edges that connect bikeshare station nodes to their nearest street intersection node in the bikeable network |
| $N_{sc}$ | Set of street intersection nodes in the scooter network |
| $A_{sc}$ | Set of street segment edges in the scooter network |
| $A_{mt}$ | Set of feeder micro-transit connector edges |
| $A_{tx}$ | Set of transfer edges |
| $N_{OD}$ | Set of origin nodes and destination nodes |
| $A_{OD,cnx}$ | Set of origin/destination connector edges |
| $W_{tx}$ | Maximum network distance between two nodes defining a transfer edge |
| $W_{OD}$ | Maximum network distance the two nodes defining an origin/destination connector edge |

- All feasible combinations of an exhaustive set of travel modes: personal vehicle, TNC, carshare, fixed-route public transit, personal bike, bikeshare, scooter, walking, and feeder micro-transit. Feasibility is achieved through topological network design and node-based movement costs.
- Multiple generic travel costs: monetary cost, mean travel time, (un)reliability, crash risk, and discomfort
- Time dependency: minute-level evaluations
- Heterogeneous traveler groups: differences in cost sensitivities

We specify that our network model allows for paths that allow for any practical combination of the allowable modes. Multiple traveler disutility factors are incorporated through a generalized travel cost function.

## 3. Methodology

The proposed process of conducting O-D routing analysis in a multimodal network includes three stages: (1) design a multimodal network model inclusive of all mobility options, (2) define a generalized cost function and determine the cost of each node and edge in the network, and (3) find the time-dependent least-cost path between any O-D pair based on traveler characteristics. The first two steps are described in the remainder of the Methodology section, and the final step is demonstrated with experiments in Section 4.3. Table 3 specifies the notation used in this paper.

### *3.1. Multimodal network design*

The first step to constructing a multimodal network model is to represent each unimodal transportation network as a graph consisting of nodes and edges. This work considers an exhaustive set of travel modes: personal vehicle, TNC, carshare, fixed-route public transit, personal bike, bikeshare, scooter, walking, and feeder micro-transit. The set of all modes, with the exception of the walking and feeder micro-transit modes, included in the multimodal network is denoted by $\mathcal{M}$. The unimodal network for each travel mode $m \in \mathcal{M}$ is separately represented by a graph $G_m = (N_m, A_m)$, where $N_m$ and $A_m$ are the set of graph nodes and edges, respectively, associated with mode $m$.

Although all unimodal networks exist physically on the same plane, they must be modeled individually as graphs and connected by transfer edges to support multimodal route-finding (Zhang et al., 2011). Transfer edges join the unimodal graphs at relevant nodes where transfers among modes can feasibly take place, which results in a single routable multimodal graph, or "supernetwork" (Carlier et al., 2002; Liao et al., 2010; Zhang et al., 2011). Origin/destination connector edges connect the origin/destination nodes to the unimodal graphs, representing a trip's network ingress/egress, respectively. The walking and feeder micro-transit networks are associated with precomputed transfer edges and origin/destination connector edges; hence, they are not modeled explicitly by their own graphs.

The subsequent section explains the process of constructing each unimodal graph $G_m$ for $m \in \mathcal{M}$. For visualization, we show a toy transportation network in Fig. 1 and its associated unimodal graph models in Fig. 2.

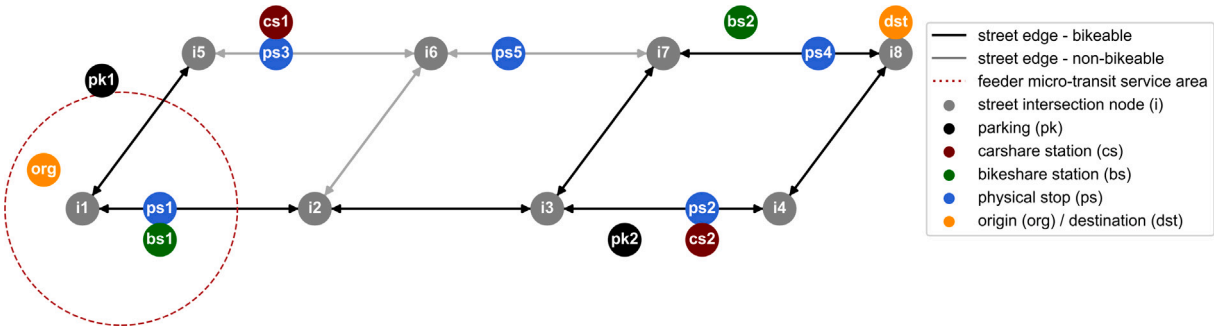


**Fig. 1.** A toy transportation network comprised of 8 street intersection nodes and 20 directional street segments, in addition to other important nodes such as carshare stations, parking spots, bikeshare stations, and transit stops. Feeder micro-transit also operates within a service area.

### 3.1.1. Unimodal graph models

The graph topology of each mobility option is discussed below:

*Personal Vehicle*. The personal vehicle network is modeled by a graph, $G_{\text{personal\_vehicle}} = (N_{dr}, N_{pk}, A_{dr}, A_{pk,cnx})$, representing the drivable street network as well as parking locations. Street intersection nodes, $N_{dr}$, comprise the graph's core set of nodes, which are connected by street segment edges, $A_{dr}$. A bidirectional parking connector edge in the set $A_{pk,cnx}$ joins each parking node in the set $N_{pk}$ to the nearest street intersection node in the set $N_{dr}$.

*TNC*. The TNC graph, $G_{\text{TNC}} = (N_{dr}, A_{dr})$, models the drivable street network. It is assumed that riders can enter or exit a TNC vehicle at any node in the network. If there is a designated pickup/drop-off point, it can be treated as a separate node. The waiting time for a TNC vehicle is embedded in the cost of transfer edges and origin connector edges. These edges represent transfers and ingress to the TNC network.

*Carshare*. Commuters using a carshare vehicle, which must be picked up at a carshare station, use the drivable network along with parking nodes for any intermediate parking. Thus, the carshare network is modeled as $G_{\text{carshare}} = (N_{dr}, N_{pk}, N_{css}, A_{dr}, A_{pk,cnx}, A_{css,cnx})$. In this model, $N_{css}$ specifies the set of all carshare stations and $A_{css,cnx}$ denotes the set of bidirectional connector edges that join the each station in the set $N_{css}$ to its nearest street intersection node in the set $N_{dr}$.

*Fixed-Route Public Transit*. The fixed-route public transit graph, $G_{\text{public\_transit}} = (N_{ps}, N_{rt}, A_{board}, A_{alight}, A_{rt})$, is modeled by the time-dependent graph presented in Ni et al. (2015). The time-dependent model of public transit was selected over the time-expanded model for its smaller size and easier integration with other unimodal graphs (Pyrga et al., 2008). In this graph, there are two sets of nodes: the physical stop node set, $N_{ps}$, and the route node set, $N_{rt}$. A physical stop node represents a physical location in the network where a bus (or subway, train, ferry, etc.) stop exists. A route node is a virtual node tied to stop node, representing a specific directional transit line associated with the stop node. Since more than one transit line can pass through one physical stop, each stop is linked to one or more route nodes. In Fig. 2, transit routes A and B both pass through physical stop 5.

The graph $G_{\text{public\_transit}}$ has three types of edges. A route traversal edge in the set $A_{rt}$ connects two route nodes if their associated physical stops are consecutive stops for a specific transit line. For example, physical stops 3 and 5 are consecutive stops for transit route A; hence route nodes 3 A and 5 A are connected by a route edge. An edge from a physical stop node to a route node, which is an element of the set $A_{board}$, represents the cost of waiting and boarding. Waiting time cost reflects the difference between the next vehicle arrival time and one's arrival time at the stop. An edge from a route node to a physical stop node, which is an element of the set $A_{alight}$, represents the cost of alighting. It is possible to change routes at one physical stop by using an alighting edge tied to one route node and a boarding edge tied to a different route node. This is demonstrated in Fig. 2 by the allowable transfer from transit route A to transit route B via physical stop 5. As seen in the supernetwork of Fig. 3(a), the model can also capture walking transfers, such as the one between physical stops 2 and 4, to be discussed in Section 3.1.2.

*Personal Bike*. The personal bike graph, $G_{\text{personal\_bike}} = (N_b, A_b)$, models the region's biking network, which includes any street segments permissible to bikes and bikeable sidewalks or trails. These segments can be determined by city rules (e.g., roads with a speed limit less than or equal to 35 miles per hour).

*Bikeshare*. The bikeshare graph, $G_{\text{bikeshare}} = (N_b, N_{bss}, A_b, A_{bss,cnx})$, consists of bikeable street edges in addition to any bikeshare station nodes and their connector edges. The station nodes represent the locations where travelers can pick up or drop off a shared bike. We assume that the supply of shared bikes is always sufficient to meet demand. A bidirectional bikeshare connector edge joins each station node in the set $N_{bss}$ to its nearest neighbor bikeable street intersection node in the set $N_b$, similar to how parking and carshare station connector edges are constructed.

*Scooter*. The scooter network, represented by the graph $G_{\text{scooter}} = (N_{sc}, A_{sc})$, is a subset of the biking network that is permissible to scooters. City regulations determine which street segments are included in the subset. For example, some city regulations maintain that scooters can only be used on streets with a speed limit less than or equal to 25 miles per hour. Unlike shared cars or bikes, scooters may be left in any valid scooter parking spot in the network. Consequently, it is not possible to model exact locations of scooter pickup and drop-off nodes. Nor is it necessary to identify these exact points, since this modeling framework is designed for planning purposes as opposed to real-time navigation. Instead, data can be used to estimate the distance distribution from

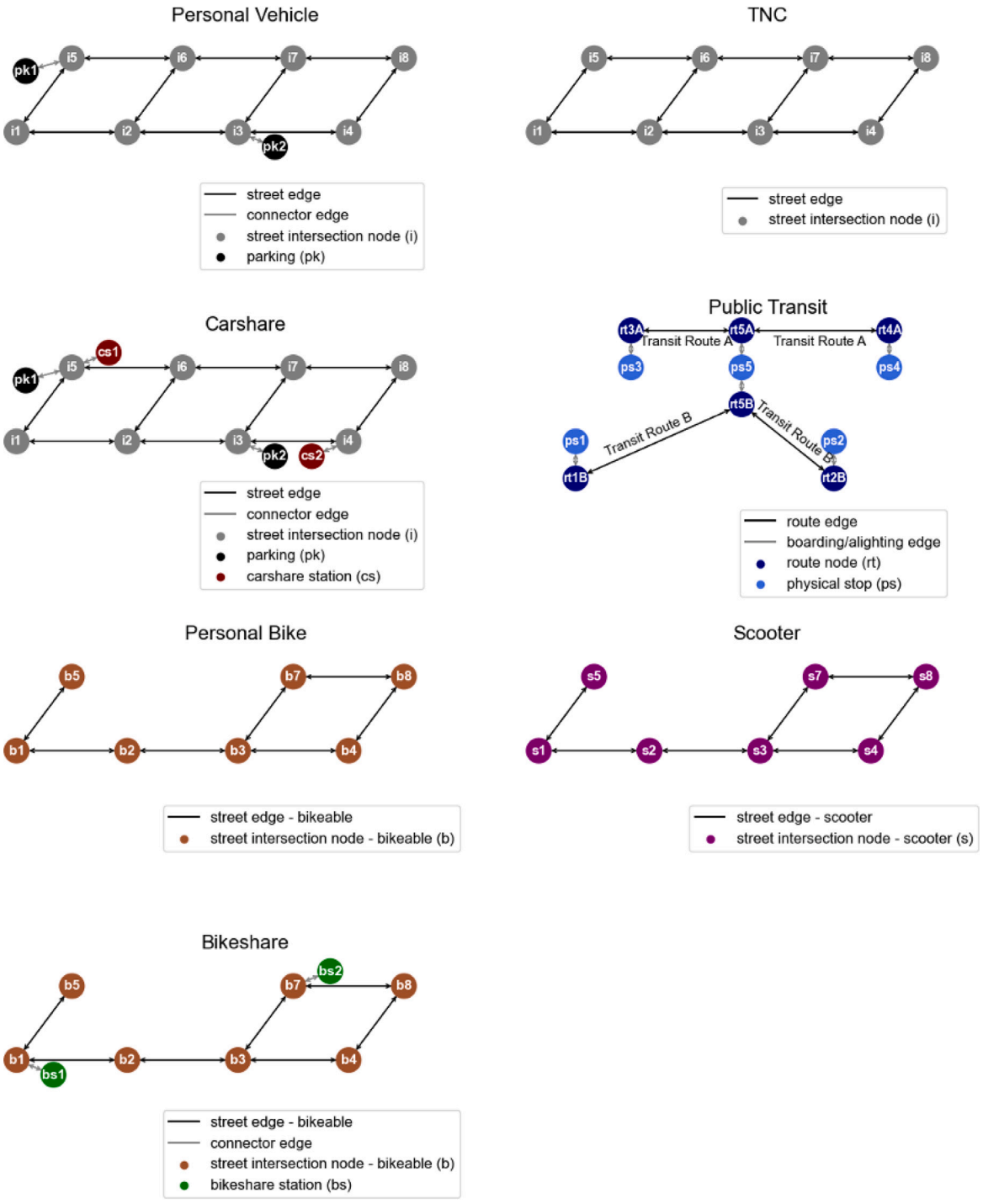


**Fig. 2.** The unimodal graph model for each travel mode $m \in \{\text{personal\_vehicle}, \text{TNC}, \text{carhare}, \text{public\_transit}, \text{personal\_bike}, \text{bikeshare}, \text{scooter}\}$.

any network node to the nearest scooter. This estimation process, which is embedded in the procedure for building transfer and origin/destination connector edges, is explained in Section 3.1.2.

*Walking.* The walking network is not explicitly modeled as its own unimodal graph; only precomputed "shortcut" walking edges are included. A shortcut edge between two nodes represents the shortest path between them, which our model approximates as the network distance between the nodes. The network distance between two nodes is estimated as their Haversine distance adjusted by a circuity factor that relates Euclidean distance to network distance. A study by Giacomin and Levinson (2015) provides average

**Table 4**
Permitted mode changes.

| Mode 1 | | Mode 2 |
|---|---|---|
| Public transit | ↔ | Public transit |
| Public transit | ↔ | Bikeshare |
| Public transit | ↔ | TNC |
| Public transit | ↔ | Personal bike |
| Public transit | ↔ | Scooter |
| Public transit | ↔ | Carshare |
| Public transit | ↔ | Personal vehicle |
| Public transit | ↔ | Feeder micro-transit |
| TNC | ↔ | Bikeshare |
| TNC | ↔ | Carshare |
| TNC | ↔ | Scooter |
| Personal vehicle | ↔ | TNC |
| Personal vehicle | ↔ | Bikeshare |
| Personal vehicle | ↔ | Scooter |
| Bikeshare | ↔ | Scooter |
| Bikeshare | ↔ | Carshare |
| Bikeshare | ↔ | Feeder micro-transit |
| Scooter | ↔ | Carshare |
| Carshare | ↔ | Feeder micro-transit |
| Walk | ↔ | *Any mode* |

circuity factors for 51 metropolitan areas, and it has also been shown that Euclidean and Haversine distances are approximately equal for small distances (Maria et al., 2020). We acknowledge that this modeling decision may introduce error in cases where two nodes are not easily reachable within the walking network, such as when they are separated geographically by a body of water or a highway. A future development could incorporate the full walking network depending on the availability of granular sidewalk data. Walking edges include the following: (1) transfer edges in the set $A_{tx}$ that define transfers between two nodes in different unimodal networks (see Section 3.1.2), and (2) origin/destination connector edges in the set $A_{OD,cnx}$ that define network ingress and egress (see Section 3.1.3). This approach mimics that of Ye et al. (2021).

*Feeder Micro-transit*. We define feeder micro-transit as a demand-responsive service that operates within a zone to connect people to/from fixed points in the network. Physical transit stops, bikeshare stations, carshare stations, origins, and destinations are the fixed nodes considered for this task. The feeder micro-transit network is incorporated into the supernetwork model in a manner similar to the walking network. First, the service zones are defined. Then, directed edges connecting any two relevant fixed nodes in the zone are added. These edges form the set $A_{mt}$.

*Other Modes*. As cities introduce other mobility modes, they can be added to the network model. These include flex-route transit and e-bikes. Flex-route transit is a combination of fixed-route and demand-responsive transit, where a vehicle makes required stops at designated checkpoints but can deviate from the general route to collect passengers in the service area (Zheng et al., 2019). This can be modeled as somewhat of a "hybrid TNC" network, where designated pickup/drop-off nodes complement the rest of network's flexible pickup/drop-off nodes. The onset of e-bikes could lead to the introduction of two separate graphs: an e-bike bikeshare graph and an e-bike personal bike graph. These graphs would replicate the bikeshare and personal bike graphs topologically, but their edge costs would be different.

### *3.1.2. Transfer edges*

After modeling each unimodal network as a graph, transfer edges are created to connect them (see Fig. 3(a)). The process is necessary so that is possible to construct a path that crosses different unimodal graphs. Transfer edges that form the set $A_{tx}$ are directional and assumed to be traversed by walking. Nodes in a unimodal graph where a mode change may take place are called switch points, following the approach of Liu (2010). If the switch point is at a predetermined location (e.g physical bus stop, bikeshare station, parking node), it is denoted as a "fixed pickup" or "fixed drop-off" node; if the switch point changes depending on the traveler's needs (e.g., TNC pickup/drop-off, scooter pickup/drop-off), it is denoted as a "flexible pickup" or "flexible drop-off" node. Each transfer edge is constructed by joining a switch point in one unimodal graph to a switch point in another.

Building transfers efficiently requires the specification of constraints on allowable changes between travel modes. Table 4 enumerates the plausible mode changes, where the arrows indicate the direction of the change. This list of allowable changes between modes is based on practical considerations. One such assumption is that travelers using a carshare vehicle can switch from the carshare mode to another mode only after leaving the vehicle in a parking zone. In addition, changing modes from personal bike to public transit is enabled by the presence of a bike rack on a bus. It is also assumed that safe intermediate bike parking is not available and bike racks do not exist on other vehicles. This implies that travelers who ride their personal bike on any part of a path can only use a combination of the personal bike, public transit, and walking networks.

Transfer edges are constructed according to the process of Algorithm 1. The network model, like the one proposed by Fan et al. (2022), assumes that travelers are willing to walk a distance less than or equal to $W_{tx}$ when transferring modes. The implication is that, for each fixed drop-off node in a unimodal network, there exists a "walking catchment zone" (WCZ) that contains all surrounding pickup nodes within a network distance of $W_{tx}$. Transfer edges are constructed between the fixed drop-off node and

**Algorithm 1** Construct transfer edges

```
Identify M_p, the set of modes characterized by flexible pickup nodes
Identify M_d, the set of modes characterized by flexible drop-off nodes

Identify N_1, the set of fixed drop-off nodes in all unimodal graphs
for n_1 ∈ N_1 do
    m_1 ← mode associated with n_1
    C_1 ← set of nodes whose distance from n_1 is less than or equal to W_tx
    Identify set of fixed pickup nodes N_2 ⊆ C_1
    for n_2 ∈ N_2 do                                  ▷ fixed drop-off to fixed pickup transfers
        m_2 ← mode associated with n_2
        if mode change permitted from m_1 to m_2 then
            Construct transfer edge from n_1 to n_2
        end if
    end for
    for m_p ∈ M_p do                                  ▷ fixed drop-off to flexible pickup transfers
        if mode change permitted from m_1 to m_p then
            n_p ← flexible pickup node in G_{m_p} nearest to n_1
            if n_p ∈ C_1 then
                Construct transfer edge from n_1 to n_p
            end if
        end if
    end for
end for

Identify N_3, the set of fixed pick-up nodes in all unimodal graphs
for n_3 ∈ N_3 do
    m_3 ← mode associated with n_3
    C_3 ← set of nodes whose distance from n_3 is less than or equal to W_tx
    for m_d ∈ M_d do                                  ▷ flexible drop-off to fixed pickup transfers
        if mode change permitted from m_d to m_3 then
            n_d ← flexible drop-off node in G_{m_d} nearest to n_3
            if n_d ∈ C_3 then
                Construct transfer edge from n_d to n_3
            end if
        end if
    end for
end for
```

each fixed pickup node within its WCZ, provided the mode change is permitted. This approach contrasts with Li et al. (2020), who assume that passengers always choose to transfer from a facility (e.g. bus stop, bikeshare station, etc.) in one unimodal network to the nearest facility in another. Our method does not impose such an assumption, allowing for routes in which travelers walk to farther facilities to complete a transfer if deemed optimal by the shortest path algorithm. This may occur in cases when the disutility of waiting for transit at one stop is higher than the disutility of walking to the next stop. For flexible drop-off nodes in the TNC, personal bike, and scooter unimodal graphs, no such WCZ exists. The reason is that travelers would logically always choose the flexible drop-off node nearest the next pickup node they desire to use. Thus, if the transfer is allowed, a transfer edge is constructed from the flexible drop-off node nearest to each fixed pickup node. The reverse situation is also true, such that transfers are built from fixed drop-off nodes to the nearest flexible pick-up node.

Our approach to building transfer edges is modeled after Delling et al. (2009), who precompute distances between two nodes that could feasibly define a transfer. We apply this same principle, thereby reducing the size of the multimodal graph by removing the walking network that is used for modal transfers. In some previous research, transfer edges are created by joining switch points in one unimodal graph to their nearest neighbor in the walking network (Dibbelt et al., 2015; Zhang et al., 2011). Constraints relating to the mode sequence are then enforced at runtime by using a specific label-constrained algorithm or only a subset of unimodal graphs. The approach in this paper is different because transfer edges, in conjunction with node costs, embed mode sequence constraints. This eliminates the need to use a label constrained shortest path algorithm. Instead, we can use the Decreasing Order of Time algorithm (Chabini, 1998) to find the shortest path between an O-D for all departure times with a single algorithm run, which has superior computational efficiency in large-scale networks.

One limitation of the network topology model is its handling of transfers to and from the personal bike graph $G_{\text{personal\_bike}}$. The reason is that, per Table 4, transfers are permitted from the personal bike mode only to the public transit mode, but transfers from

the public transit mode are permitted to any other mode $m \in \mathcal{M}$. This scenario creates an issue where it is possible that a path sequentially uses the personal bike, public transit, and TNC modes, for example. However, this path is not sensible because a personal bike cannot be stored on a TNC vehicle. One solution is to run the shortest path algorithm separately on two supernetworks: (1) one that includes all modes $m \in \mathcal{M}$ except the personal bike mode, and (2) one that includes only the personal bike and public transit modes. The path with the lower generalized cost between these two options is then selected as the optimal path. Alternatively, we could assume that intermediate bike parking exists at various points in the network. In this case, we would permit transfers between the personal bike mode and all other modes. A path that sequentially personal bike, public transit, and TNC modes would thus be allowed.

#### 3.1.3. O/D connector edges

The set of origin and destination nodes is denoted by $N_{OD}$. Each origin/destination is connected to pickup/drop-off nodes in the unimodal graphs by O/D connector edges, respectively. The set of O/D connector edges, denoted by $A_{OD,cnx}$, represents a trip's ingress to/egress from the multimodal network (Fan et al., 2022).

The procedure to create O/D connector edges is similar to the process of creating transfer edges. To build origin connectors, a WCZ around the origin is constructed. The origin's WCZ contains the set of pickup nodes whose network distance from the origin is less than or equal to $W_{OD}$. An origin connector edge is then added from the origin to each fixed pickup node within the WCZ. For a graph with flexible pickup nodes (e.g., TNC, personal bike, scooter), a single origin connector edge joins the origin to the nearest flexible pickup node in the graph. This full process is repeated for destination connector edges, with edges instead added from fixed/flexible drop-off nodes to the destination node.

#### 3.1.4. Feeder micro-transit connector edges

For completeness, we repeat here that directed feeder micro-transit connector edges join any two relevant fixed nodes in the feeder service zone. These edges form the set $A_{mt}$. The fixed nodes connectable by feeder micro-transit are physical transit stops, bikeshare stations, carshare stations, the origin, and the destination.

#### 3.1.5. Supernetwork

The multimodal graph $G_{MM}$ is defined as the union of all unimodal graphs, transfer edges, origin and destination nodes, O/D connector edges, and feeder micro-transit connector edges:

$$G_{MM} = \bigcup_{m \in \mathcal{M}} G_m \bigcup A_{tx} \bigcup N_{OD} \bigcup A_{OD,cnx} \bigcup A_{mt} \tag{1}$$

Fig. 3(a) displays an example supernetwork with mode set $\mathcal{M} = \{\text{TNC}, \text{public\_transit}, \text{bikeshare}\}$, based on the original network shown in Fig. 1. We display a smaller mode set for visualization clarity. The walking and feeder micro-transit modes are included via precomputed transfer edges, O/D connector edges, and feeder micro-transit connector edges. The supernetwork of Fig. 3(a) is routable, meaning that it is possible to find a connected route that starts at the origin and ends at the destination. Specifically, the supernetwork permits multimodal paths, such as the one shown in Fig. 3(b).

### 3.2. Cost assignment

After defining the graph topology of the supernetwork, a time-dependent travel disutility is assigned to each edge and node. However, it is important to note that the topology is still independent of any learned disutility function. The total disutility of travel, also named the generalized travel cost, is estimated by the weighted sum of mean travel time, monetary cost, (un)reliability, risk, and discomfort. (Un)reliability will herein be referred to as "reliability." The step of assigning generalized travel costs to the multimodal network precedes any routing analysis.

#### 3.2.1. Generalized travel cost function

The proposed method defines a generalized travel cost function for each edge that is a combination of five time-dependent decision attributes: monetary cost, mean travel time, reliability, crash risk, and discomfort. This function is designed to encapsulate interpretable and measurable factors that have been shown to influence traveler behavior (Vredin Johansson et al., 2006). In Section 4.2, we explain the data gathering procedure for each attribute.

The generalized travel cost, $GTC_e(t)$, of an edge $e$ as a function of edge entry time $t$ is given by Eq. (2):

$$GTC_e(t) = \beta_x \cdot c_e^x(t) + \beta_T \cdot c_e^T(t) + \beta_r \cdot c_e^r(t) + \beta_k \cdot c_e^k(t) + \beta_D \cdot c_e^D(t) \tag{2}$$

where $c_e^x(t), c_e^T(t), c_e^r(t), c_e^k(t), c_e^D(t)$ denote the monetary cost, mean travel time, reliability measure, crash risk measure and perceived discomfort measure of edge $e$ when entering the edge time $t$, respectively.

In the generalized cost function of Eq. (2), each of the five cost factors is weighted by a $\beta$ parameter to account for heterogeneity across traveler groups (Du and Wang, 2014). These parameters can be interpreted as the dollar value that a person assigns to a single unit of the corresponding cost factor. The parameter $\beta_x$ thus takes on the unitless value of 1, while $\beta_T$ has units of dollars per time unit and is representative of a person's value of average travel time. The $\beta$ parameters can be determined based on the specific population group under consideration or the goals of the transportation planner, and our implementation allows for such flexibility. For example, a planner interested in bike safety may choose to give a higher weight to $\beta_k$ to identify more favorable routes for

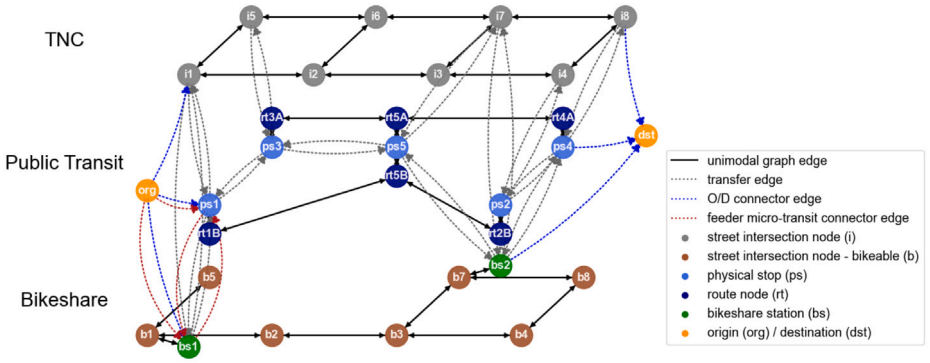


(a) The supernetwork model for $m \in \{\text{TNC}, \text{public\_transit}, \text{bikeshare}\}$, one origin, and one destination. The walking and feeder micro-transit modes are included via precomputed transfer edges, O/D connector edges, and feeder micro-transit connector edges. The unimodal graphs are slightly offset for visualization purposes since they physically overlap.

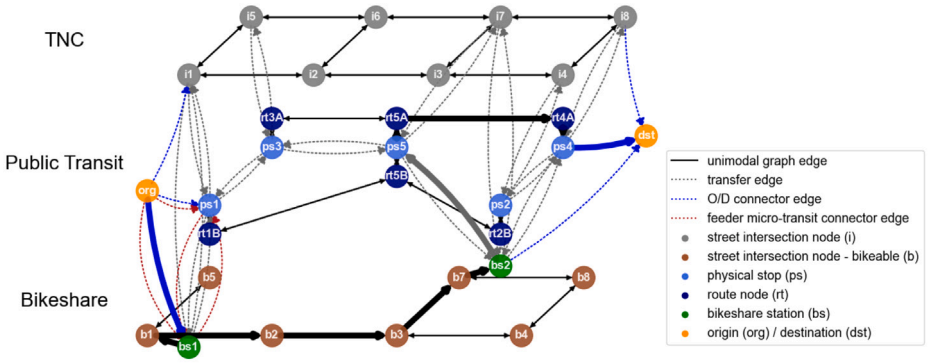


(b) A multimodal path (bolded) consisting of bikeshare, public transit, and walking (for transfer and O/D connector edges).

**Fig. 3.** An example supernetwork and permissible multimodal path.

cyclists. A planner may also choose to assign a higher value of time $\beta_T$ when evaluating route options during commuting hours as opposed to off-peak hours.

The monetary cost of an edge, $c_e^x(t)$, is calculated as the sum of the fixed and operational fees (per-minute and/or per-mileage fees) required to use the edge. Fixed transit fares are counted only once since they are stored within transit boarding edges. Similarly, fixed scooter-unlock fees and TNC base fares are embedded within origin connector and transfer edges directed toward the scooter and TNC unimodal graphs, respectively. Traversal edges store the edge's corresponding minute- and/or distance-based operational fees.

Mean travel time, $c_e^T(t)$, is defined as the day-to-day average travel time (inclusive of both waiting and traversal time) required by an edge $e$ at entry time $t$. Eq. (3) provides the calculation:

$$c_e^T(t) = \begin{cases} \frac{l_e}{s_e}, & \text{if } e \in A_b, A_{bss,cnx}, A_{sc}, A_{tx}, A_{OD,cnx} \\ \frac{l_e}{\alpha_e(t) \cdot s_e}, & \text{if } e \in A_{dr}, A_{pk,cnx}, A_{css,cnx}, A_{mt} \end{cases} \tag{3}$$

where $l_e$ is the length of edge $e$ and $s_e$ is the free-flow speed of the mode associated with edge $e$. For edges associated with active mode graphs (e.g., personal bike, bikeshare, scooter, walking), the free-flow speed is given by the mode's average movement speed, which is based on previous research (Jensen et al., 2010; Almannaa et al., 2021; McCrum et al., 2019). The free-flow speed of active mode edges is assumed to persist throughout the day, regardless of traffic conditions. We do not consider the effect of terrain elevation on micromobility speeds, though such analysis could feasibly be conducted in future work. For edges associated with

non-transit vehicle mode graphs (e.g., personal vehicle, TNC, carshare), the free-flow speed is the edge's speed limit. The free-flow speed of non-transit vehicle mode edges is assumed to vary throughout the day in accordance with traffic flow. Thus, the free-flow speed of these edges is adjusted by an edge-specific time-of-day multiplier, $\alpha_e(t)$, which can be calibrated on the level of road class using intraday vehicle speed data (provided by INRIX, HERE, TomTom, or Google Maps, for example).

We clarify that network edges involving the public transit mode are not represented in Eq. (3) since waiting and in-vehicle times are determined by the General Transit Feed Specification (GTFS) schedule. The average waiting time associated with a boarding edge in the set $A_{board}$ reflects the difference between the next vehicle arrival time per the schedule and one's arrival time $t$ at the stop. The average in-vehicle time associated with a route edge in the set $A_{rt}$ is extracted from the schedule. Alighting edges in the set $A_{alight}$ are assigned a travel time representative of the typical time to alight a transit vehicle. To account for systematically high traffic times, we also adjust the average waiting and in-vehicle time by the multiplier $\alpha_e(t)$ depending on edge entry time $t$.

Researchers have proposed a variety of metrics to measure travel time reliability that reflects day-to-day variation (Pu, 2011). We choose an edge's 95th percentile travel time, denoted by $c_e^r(t)$, for the reliability metric since it is easily interpretable. An edge's 95th percentile travel time is estimated as the product of its mean travel time $c_e^T(t)$ and a scalar multiple $\lambda_e(t)$ that relates the two values:

$$c_e^r(t) = \lambda_e(t) \cdot c_e^T(t) \tag{4}$$

For edges associated with vehicle mode graphs (e.g., personal vehicle, TNC, carshare, public transit), $\lambda_e(t)$ can be calibrated on the level of road class using probe vehicle speed data that provides intraday travel time variation. It is indeed possible to calculate $\lambda_e(t)$ on the edge-level, though such detailed data may be difficult to obtain. Transit on-time performance data can be used to estimate $\lambda_e(t)$ for boarding edges in the set $A_{board}$ that embed waiting time. We assume that travel time does not vary for edges associated with active mode graphs (e.g., personal bike, bikeshare, scooter, walking); this implies that $\lambda_e(t)$ for active mode edges is 1, and both the 95th percentile and mean travel times of these edges are equivalent.

Regarding the relationship between $c_e^T(t)$ and $c_e^r(t)$, we note that they are indeed correlated. Thus, the relative weighting between $\beta_T$ and $\beta_r$ is important in determining to what degree the specific traveler group prioritizes average travel time over the 95th percentile travel time, and vice versa. It is certainly possible to keep only one of the attributes by assigning a zero value to the $\beta$ parameter associated with the other attribute. A transportation planner could also adopt a different definition of reliability, such as the 75th percentile or 85th percentile travel times. Our model and its implementation allow for such flexibility.

Following common practice in safety engineering (DiGioia et al., 2017), an edge's risk measure $c_e^k(t)$ is defined as its crash risk at time $t$. The crash risk along an edge $e$ is estimated as the predicted daily count of vehicle crashes on the edge, adjusted by two scalar multipliers: (1) $k_e$, the national crash rate of the mode associated with edge $e$ relative to the national vehicle crash rate according to National Household Travel Survey data (Beck et al., 2007), and (2) $F_e$, a crash modification factor (CMF) between zero and one that accounts for bikeway infrastructure along the edge. The CMF depends on the type of bikeway infrastructure. CMFs are available from a previous study (Dadashova, 2022). Eq. (5) provides the risk calculation:

$$c_e^k(t) = c_e^k = \hat{y}_e \cdot k_e \cdot F_e \tag{5}$$

where $\hat{y}_e$ is the predicted daily count of vehicle crashes along edge $e$ according to a Poisson regression model. The reason this model predicts vehicle crashes instead of bicycle, scooter, or walking crashes directly is due to more reliable reporting of vehicle incidents. This paper assumes a crash risk model of the form $\log(y_e) = \beta_0 + \beta_l \cdot l_e + \beta_{rc} \cdot rc_e + \beta_s \cdot s_e + \varepsilon_e$, where $y_e$ is the expected value of the edge's crash count, $l_e$ is the edge's length, $rc_e$ is the edge's road class, and $s_e$ is the edge's speed limit. The crash risk of an edge is assumed to be time-independent, though it is theoretically possible to construct the regression on a time-of-day level of detail. The $\beta$ parameters of the regression, which are distinct from the parameters of Eq. (2), are estimated by observed vehicle crash data specific to the study area.

A discomfort metric is also included in the generalized travel cost to account for discrepancies in physical effort by travel mode. We conceptualize the discomfort index as a mode-specific preference value that reflects the difficulty or inconvenience associated with a particular mode, based on previous research indicating that user mode preference is a notable factor in path selection (Liu et al., 2021; Yang et al., 2024). The discomfort of an edge $e$ is defined by its perceived physical discomfort, which is measured by the edge's length multiplied by a physical discomfort index $d_e$, shown in Eq. (6):

$$c_e^d(t) = c_e^d = d_e \cdot l_e \tag{6}$$

The discomfort index $d_e$ depends on the mode associated with edge $e$. To derive index values, we normalize the results of a previous work's survey that asked participants to state the mode choice of their daily commute and rate the physical effort required (Gatersleben and Uzzell, 2007). We acknowledge that calibrating these values using more advanced models could be the subject of future work.

For a more detailed presentation of the data used to calibrate and assign parameters used by Eqs. (3), (4), (5), and (6), see Tables 5 and 6 in Section 4.2.

#### 3.2.2. Costs of transfer edges, O/D connector edges, and feeder micro-transit connector edges

Transfer and O/D connector edges are traversed by walking. As described in Section 3.1.1, each of these edges represents the shortest walking path between the two nodes that define the edge. The length of the shortest path is estimated as the Haversine distance multiplied by a circuity factor that relates Euclidean distance to network distance (Giacomin and Levinson, 2015). The pedestrian crash risk of these walking edges is estimated by assuming values for road class and speed limit. Then, we can calculate

**Table 5**
Specification of mode-dependent parameters used for Pittsburgh case studies.

| Mode of edge $e$ | Monetary cost | Speed $s_e$ | Crash risk index $k_e$ | Discomfort index $d_e$ |
|---|---|---|---|---|
| Public transit | $2.75/ride + $0.00/min + $0.00/mile | N/A[a] | 0.19 | 1.66 |
| Bikeshare | $0.00/ride + $0.125/min + $0.00/mile | 14.5 km/h | 1.81 | 2.43 |
| Scooter | $1.00/ride + $0.39/min + $0.00/mile | 10.0 km/h | 1.81 | 2.43 |
| Carshare | $0.00/ride + $0.183/min + $0.00/mile | Speed limit | 1.0 | 1.0 |
| TNC | $6.67/ride[b] + $0.19/min + $1.12/mile | Speed limit | 1.0 | 1.0 |
| Walk | $0.00/ride + $0.00/min + $0.00/mile | 4.7 km/h | 0.28 | 2.13 |

[a] Speed not needed because travel time gathered from GTFS schedule.
[b] Reflects the base fare, booking fee, and a minimum fare buffer.

**Table 6**
Specification of additional parameters used for Pittsburgh case studies.

| Parameter | Value |
|---|---|
| Parking length of time | 8 hours |
| Parking expense per hour | $2.50/h |
| CMF, protected bike lane | 0.425 |
| CMF, unprotected bike lane | 0.554 |
| CMF, trail | 0.425 |
| CMF, bikeable sidewalk | 0.554 |
| Transfer inconvenience cost | 2 min |
| TNC average waiting time | 6 min |
| TNC 95th percentile waiting time | 12 min |
| $W_{tx}$ | 0.50 miles |
| $W_{OD}$ | 0.60 miles |

the cost attributes of these edges using Eq. (3), (4), (5), and (6). A travel time-based inconvenience cost is also added to each transfer edge to penalize transfers.

The length of each feeder micro-transit connector edge is estimated in the same way. Assuming the availability of historical data on micro-transit trips such as that provided by Liezenga et al. (2024), we can estimate the mode's average speed and also evaluate a reliability metric. Waiting time is embedded within the travel time. To calculate crash risk, we assume a single road class value for each edge.

### 3.2.3. Node costs

In addition to edge costs, the model incorporates movement-based node costs. Node costs are imposed to either penalize or benefit movement from one edge to another edge via a specific node. We can account for fee-less or discounted transfers in this way. Consider the toy supernetwork shown in Fig. 3(a) and assume that transit requires a fixed fare of $2.75. This fare is included within all boarding edges (those directed from a physical stop to a route node). To ensure free transfers within the transit network, we add node costs to physical stop nodes if the incoming edge is an alighting edge and the outgoing edge is a walking transfer edge leading towards another physical stop node. For example, we implement $-2.75 on node 'ps5' if the incoming edge is ('rt5B', 'ps5') and the outgoing edge is ('ps5', 'ps3'). This $-2.75 value negates the positive $2.75 fare associated with the boarding edge ('ps3', 'rtA'). Hence, the path ('org', 'ps1', 'rt1B', 'rt5B', 'ps5', 'ps3', 'rt3A', 'rt5A', 'rt4A', 'dst'), which uses transit route A and transit route B with a transfer between physical stops 5 and 3, has a summative fare of $2.75. We note that one shortcoming with this approach is that we cannot properly account for fee-less transfers along paths that sequentially use transit, some other mode, and transit again. The fixed fare associated with boarding edges would be counted twice in these cases.

Conversely, positive node costs restrict transfers between two modes, which is of particular importance for modeling route options of groups such as disabled individuals who cannot use active modes. Demonstrating this case on Fig. 3(a), we can implement arbitrarily high node costs on the bikeshare station nodes if the incoming edge is a transfer or origin connector edge and the outgoing edge is a bikeshare graph traversal edge. This will effectively constrain transfers to the bikeshare network.

Positive node costs can also prohibit the usage of two consecutive transfer edges to constrain sequential walking segments whose cumulative length exceeds $W_{tx}$. This additionally imposed cost for walking edges may be trivial in practice since excessive walking is unlikely to be selected over an efficient alternative mode.

## 3.3. O-D routing analysis

After assigning costs and $\beta$ parameters, we use the multimodal network to conduct routing analysis. This entails measuring the shortest path between an O-D pair, where "shortest" in this context means the lowest generalized travel cost. We extract the generalized travel cost, along with the monetary cost, mean travel time, reliability, crash risk, and discomfort cost attributes from the identified optimal path. These attribute values can subsequently be used in accessibility calculations.

The time-dependent shortest path necessary for this analysis is found with the Decreasing Order of Time algorithm presented in Chabini (1998). This algorithm was selected because it outputs the shortest path for all departure times with a single algorithm

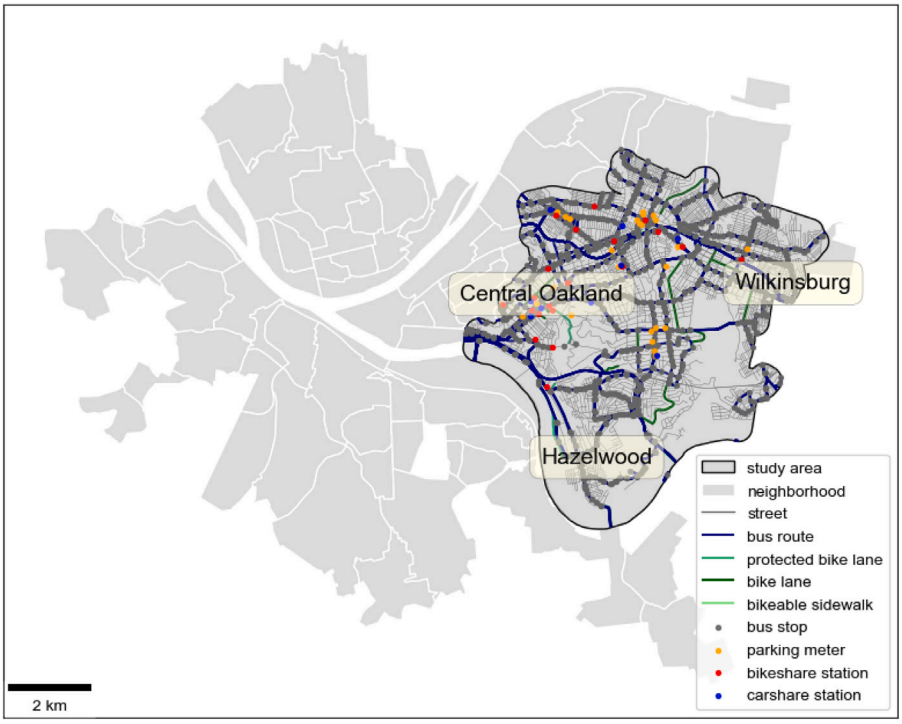


**Fig. 4.** A map display of the study area shown against the backdrop of all the neighborhoods in Pennsylvania's Allegheny County. The first three case studies focus on the Wilkinsburg-Central Oakland and Hazelwood-Central Oakland O-D pairs.

run and high computational efficiency. Its implementation in the MAC-POSTS Python package is available on Github (Ma et al., 2024) and detailed in Ma et al. (2020).

## 4. Experiments and results

To illustrate potential use cases of the proposed model and method, we conducted four case studies in Pittsburgh, PA during the morning period of 7:30 AM to 8:30 AM. The first three experiments are sensitivity analyses that reveal the effects of the following model elements on the shortest path between selected O-D pairs: (1) minute-level departure time, (2) $\beta_T$ (value of mean travel time) in Eq. (2), and (3) usage pricing of shared scooters. The first experiment also compares the path selected by NOMAD versus the path selected by r5r. In the fourth case study, we calculate the cumulative opportunities metric of accessibility for all origins in a public transit/walking supernetwork versus a public transit/bikeshare/walking supernetwork. Importantly, we do not claim that the routes deemed optimal by NOMAD are in fact what travelers select; instead, we state only that these routes are theoretically optimal given the assumed generalized cost function, assumed traveler cost sensitivities, and data with which the model is calibrated.

### *4.1. Study context*

The method was demonstrated on the transportation network of 19 demographically-different neighborhoods in Pittsburgh, PA. The study area is depicted in Fig. 4. In the Pittsburgh region, Zipcar runs the carsharing service, POGOH operates the bikeshare system, Spin managed the scooter fleet from 2021–2023, Uber and Lyft operate TNC vehicles, and Pittsburgh Regional Transit acts as the public transit agency. The city does not yet have a feeder micro-transit service.

In 2021, the City of Pittsburgh's Department of Mobility and Infrastructure launched a MaaS pilot called Move PGH with the intention of facilitating multimodal travel and encouraging shared mobility (City Of Pittsburgh, 2022). Move PGH leveraged public–private partnerships to expand and integrate shared vehicles, bicycles, and e-scooters with the city's public buses through on-street "Mobility Hubs" and a trip-planning app called Transit. The Move PGH initiative was designed to facilitate safe, affordable, and reliable non-vehicle travel for all households. Policymakers at the Department of Mobility and Infrastructure can use the network model to evaluate multimodal connectivity and conduct accessibility analysis. This can inform decisions on future network investments.

We included all shared modes (e.g., public transit, bikeshare, scooter, TNC, carshare) and the walking mode in the supernetwork model to replicate Pittsburgh's MaaS system. The personal vehicle and personal bicycle networks were consequently excluded in all test cases. The feeder micro-transit mode was also excluded since the city does not yet operate this service. Furthermore, we assumed that travelers are able-bodied and can use active modes of transportation. These assumptions are not required, though they are appropriate for the context of Move PGH.

### 4.2. Network settings and data

The study area's driving and biking networks were extracted from Allegheny County's street centerlines GIS data hosted on the Western Pennsylvania Regional Data Center (WPRDC). WPRDC also provided locations of bikeshare stations, bike lanes, and parking meters. For modeling simplicity, the parking nodes were consolidated into one representative node per parking zone, represented by the average location of a parking meter within a zone. The parking price for Zipcar users in our case studies was estimated as $2.50 per hour for 8 hours, totaling $20 for a workday. Locations of carshare stations were found by querying Google My Maps for Zipcar locations, since a dataset was not readily available. GTFS provided public transit stop locations and route schedules.

In total, the study area consists of 641 km of physical streets, 20 bikeshare stations, 1108 public transit stops, 93 directional bus routes, 10 carshare stations, and 1224 parking meters, as shown in Fig. 4. The full supernetwork, inclusive of all traversal, transfer, and O/D connector edges, has 18,789 nodes and 162,669 edges. A large share of these edges are transfer edges between transit stops.

As described in Section 3.2.1, the five cost attributes used to determine an edge's generalized travel cost are monetary cost, mean travel time, reliability, risk, and discomfort. Assigning these cost attributes to the edges required the specification and calibration of several parameters, which are reported in Tables 5 and 6. Usage prices for a Zipcar vehicle, POGOH bikeshare, SPIN scooter, and Pittsburgh Regional Transit bus ride were gathered from the respective company and agency websites to establish an edge's monetary cost. TNC prices were obtained by querying various Pittsburgh O-D pairs in the Uber app and viewing the price breakdown by per-minute, per-mileage, and booking fee. Speed data for active modes was gathered from previous research (Jensen et al., 2010; Almannaa et al., 2021; McCrum et al., 2019). To determine the effects of intraday and inter-day traffic conditions on speed, we used INRIX data. This data contained speed and travel time data at five-minute intervals for various road segments in the study area. GTFS provided public transit schedules, which were used to estimate mean travel time for transit edges. The 95th percentile waiting time for a transit line at a given departure time was estimated as the scheduled waiting time at the given departure time plus half of the average headway for the specific transit line. We acknowledge that this estimation is simplified due to limited availability of retrospective data. Future work may consider acquiring necessary data and adopting the methods proposed by Liu et al. (2023) or Braga et al. (2023) for a more accurate calculation of the 95th percentile waiting and in-vehicle time of transit edges. Wang and Mu (2018) provided the TNC average waiting time estimate of 6 minutes. The 95th percentile TNC waiting time was assumed to be twice the average waiting time. We gathered two years of observed vehicle crash data in the study area from WPRDC to calibrate the vehicle crash prediction model. For an edge's mode-specific crash index, we used National Highway Traffic Survey data presented by Beck et al. (2007). Crash modification factors were provided by Dadashova (2022), and the physical discomfort indices were gathered from survey data presented by Gatersleben and Uzzell (2007).

The walking transfer distance $W_{tx}$ and the O/D connection edge length $W_{od}$ were set at 0.50 miles and 0.60 miles, respectively, based on a study by El-Geneidy et al. (2014) that explored commuters' actual walking distances to their first transit stop. The value of 0.60 miles corresponds to the 95th percentile walking distance to the first stop and hence is a conservative estimate for $W_{od}$. We decreased the value of $W_{tx}$ to 0.50 miles assuming that travelers are willing to walk slightly less to transfer modes during their trip. Additionally, a 2-min inconvenience cost was added to each transfer edge's walking travel time as a soft penalty for transfers.

In the supernetwork model, a simplification is made where a transfer from a fixed drop-off node in a unimodal graph to the scooter graph occurs at the nearest scooter node in the scooter graph. This simplification ignores the fact that shared scooters are not always available at every intersection. If the model were used for real-time trip planning, a real-time API would be required to determine the actual nearest scooter location. However, for general accessibility analysis, we need only to estimate the generalized travel cost of the transfer edge leading to the scooter network. This involves estimating the average and 95th percentile distance from each fixed drop-off node to the nearest scooter based on historical observations. Since we lacked historical data, we generated a distance distribution by simulating historical observations. This process entailed uniformly randomly placing 1000 scooters in the study area over 30 days. The choice of 1000 scooters was based on statistics provided in the Move PGH report.

We ensure that our network model is a valid representation by running the shortest path problem for various O-D pairs and cross-checking the result against Google Maps. This includes checking that any public transit paths returned by our model for a given O-D pair are feasible according to Google Maps. For example, if our model indicates that the shortest path is characterized by a transfer between two bus lines, we ensure that this same path also appears in Google Maps for similar departure times. Validating multimodal paths that include transit/bikeshare/walking requires both Google Maps and domain knowledge. When NOMAD returns a transit/bikeshare/walking path for a given O-D pair, we first use Google Maps to ensure that this alternative path is reasonable. This step involves checking that the transit path is arduous in the sense that it is either characterized by long wait times, a single or double transfer, or a circuitous route. Then, we use domain knowledge to confirm that a bikeshare station is near the origin (if bikeshare is used for the first segment) or the destination (if bikeshare is used for the last segment). Furthermore, TNC paths are validated by comparing the total travel time, less any waiting time, with the total travel time of the driving mode with Google Maps. Our observations indicate that the average travel time of TNC paths within NOMAD is slightly lower than a personal vehicle's travel time according to Google Maps, even though the TNC path incorporates a 6 minute wait. This indicates that our model underestimates the in-vehicle time of TNC paths, which we attribute to two factors: (1) underestimation of traffic conditions, and (2) lack of penalty for traffic lights. These factors may be addressed through improved data quality for intraday vehicle speeds as well as implementation of node costs at traffic light intersections, respectively.

Finally, we choose reasonable values for the $\beta$ parameters based on existing studies (Li et al., 2010; Carrion and Levinson, 2012). We acknowledge that proper calibration of these values should be the subject of future work using discrete choice modeling with revealed preferences. Still, the capabilities of our model can be demonstrated with the selected $\beta$ values.

### 4.3. Case studies

The first three experiments focus on two representative O-D pairs, namely Wilkinsburg - Central Oakland and Hazelwood - Central Oakland. The Central Oakland neighborhood was chosen as the destination since it has the county's highest number of "opportunity occupations," or jobs that pay at least the average wage and do not require a Bachelor's degree (Wardrip et al., 2015; U.S. Census Bureau, 2020; U.S. Bureau of Labor Statistics, 2022; O*NET Resource Center, 2024). The Wilkinsburg and Hazelwood neighborhoods were selected as the origins for exposition because they are low-income with a high unemployment rate relative the rest of the county (U.S. Census Bureau, 2022). Policymakers aiming to improve access to jobs may seek to prioritize better transportation options for commuters traveling from Hazelwood and Wilkinsburg to Central Oakland. The fourth case study calculates accessibility for all origins in the study area, which entails constructing a multimodal O-D cost matrix that accounts for all destinations. All origins and destinations are represented by census block group centroids.

#### 4.3.1. Case study 1: Sensitivity analysis of departure time and comparison between NOMAD and r5r

The objectives of the first case study are twofold: (1) explore how minute-level changes in departure time affect path modes, average travel time, and total cost of the shortest path; and (2) compare these results with r5r. The $\beta$ parameters were set as follows: $\beta_T$ = \$10.00/h, $\beta_r$ = \$10.00/h, $\beta_x$ = \$1.00/\$1.00, $\beta_k$ = \$20.00/crash, and $\beta_D$ = \$0.00/discomfort-weighted-km. Assigning $\beta_D$ = \$0.00/discomfort-weighted-km indicates that the traveler group of interest gives no value to physical discomfort. We emphasize that the routes discovered by NOMAD are only theoretically optimal for the traveler group defined by this specific cost function.

Figs. 5(a) and 5(b) display the generalized travel cost and average travel time of the shortest path from 7:30 AM to 8:30 AM for the two O-D pairs. The optimal path for each departure time is colored by the modes that define it. The Wilkinsburg - Central Oakland O-D pair in Fig. 5(a) shows the advantages of a bikeshare system that complements the schedule-based, fixed-route public transit network. Several different bus lines pass through bus stops that are walkable from the Wilkinsburg origin, with some of these bus lines offering a direct path from origin to destination. These cases are represented by the yellow-green markers. However, infrequent service means that commuters departing from Wilkinsburg experience long waiting times for these direct bus lines depending on the departure time. In these cases, the optimal path shifts from a transit/walking route to a transit/bikeshare/walking route. These multimodal paths are identified because they have lower generalized travel costs relative to paths that involve transferring between two distinct bus routes. This is due to the fact they are more reliable since travelers do not have to wait twice. Inspecting these paths reveals that bikeshare serves as a last-mile solution, where commuters take an express bus for the longer initial segment of their trip followed by a shorter bikeshare segment at the end. The identification of these multimodal paths indicates that express bus lines are well-connected to bikeshare stations. In general, the result is that the bikeshare mode keeps the average travel time below 40 minutes for most departure times, thereby limiting any gaps in accessibility that may be caused by the transit schedule. Interestingly, there are no cases in which the optimal route uses bikeshare for the full trip. Although these routes are highly reliable in terms of travel time, we suspect such a path is never suggested for a traveler with these cost sensitivities due to the long walk time from the origin to the nearest bikeshare station.

We compare our results with those found by r5r for the Wilkinsburg - Central Oakland O-D pair during the same departure time interval. According to our testing and examined r5r source code (Pereira et al., 2024b), users can select either walking or personal bike as an access/egress mode for routing with public transit. An error message states that park-and-ride and bikeshare not supported at this time. We chose walking as the access/egress mode, meaning the path modes are always transit/walking. Results are shown in Fig. 5(c), where each point is colored by the number of distinct transit lines required. We observe that total travel time decreases linearly with an impending bus arrival, which is an expected result for a schedule-based transit network. Since the origin is located near bus stops serviced by different routes, total travel time is less sensitive to departure time. When comparing Figs. 5(a) and 5(c), we observe similarities in travel time, which hovers between 30 and 40 minutes for most times in the window. Still, differences are apparent as NOMAD determines that transit/bikeshare/walking paths are often optimal, with the transit portion including an express bus line. The difference is likely due to the generalized cost function of our model and its incorporation of a reliability term. Specifically, transit waiting time reliability at time $t$ is given by the 95th percentile waiting time, which is estimated as the waiting time at time $t$ per the GTFS schedule plus half of the average headway. This estimation occurs in the absence of real data. Because we assigned $\beta_r$ = \$10.00/h, the reliability term has a sizeable effect on the cost function. Bikeshare is part of the optimal route for many departure times because active mode travel time is assumed to have no day-to-day variation, implying a low reliability cost as measured by the 95th percentile travel time.

For commuters going from Hazelwood to Central Oakland, the optimal path mode combination is notably dependent on departure time, as shown in Fig. 5(b). In many instances, the least-cost route is characterized by TNC/walking. These cases are associated with long transit waiting times, and the TNC mode effectively serves to cap the generalized cost during these temporal gaps in transit service. We comment that only the travelers with comparably high values of mean travel time and reliability may theoretically desire such a path, since TNCs are relatively expensive in terms of monetary cost. Our model also suggests that the TNC mode is not a viable first-/last-solution, which may be attributed to a high minimum fare and lack of incentives for connecting to other modes. In addition, several departure times are associated with a transit/bikeshare/walking route, where bikeshare is used for the second segment. These multimodal paths are deemed optimal when waiting time for the bus for the first segment is short. The reason that TNC paths often replace these multimodal paths, unlike the first example, is because transit service near this origin is both spatially and temporally limited. The Hazelwood neighborhood does not have an abundance of bus lines that pass through it. Not only does this imply generally limited connectivity with destinations directly, but also limited connectivity with other modes. The ability to

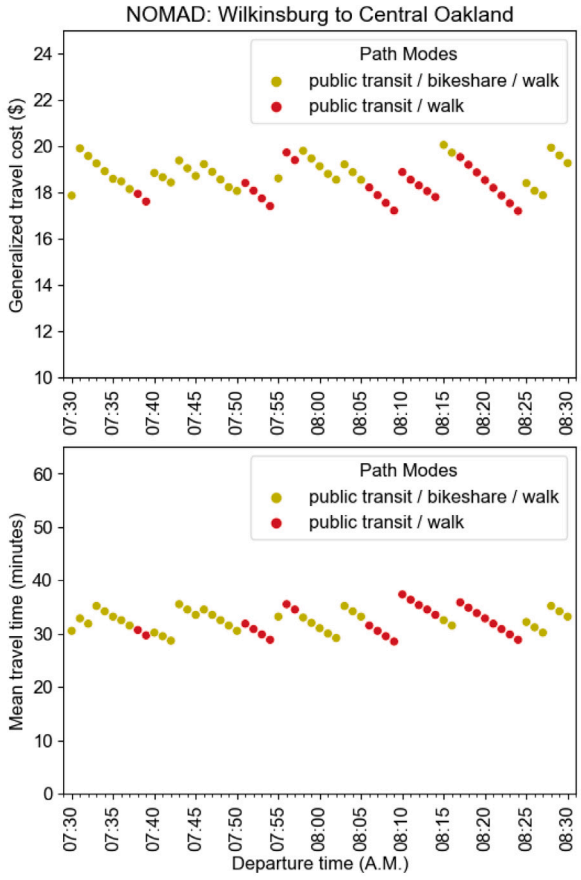


(a) NOMAD: Optimal Path from Wilkinsburg to Central Oakland.

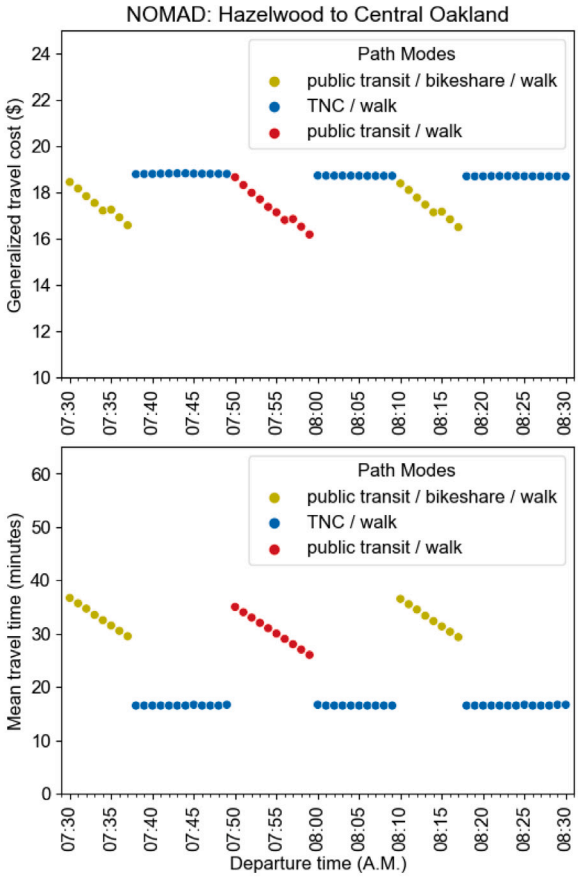


(b) NOMAD: Optimal Path from Hazelwood to Central Oakland.

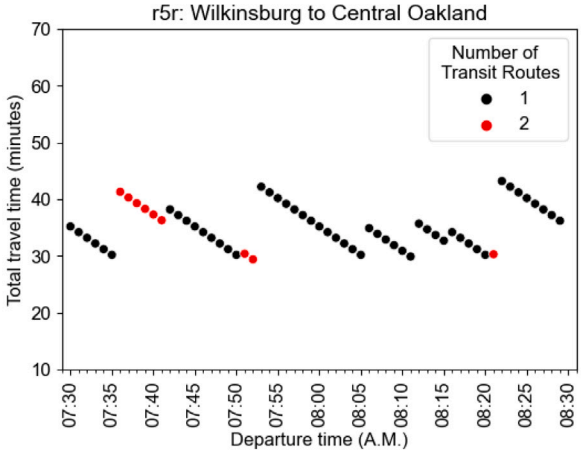


(c) r5r: Optimal Path from Wilkinsburg to Central Oakland.

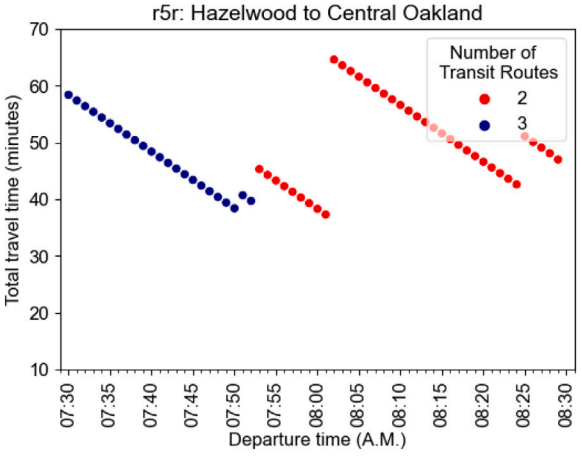


(d) r5r: Optimal Path from Hazelwood to Central Oakland.

**Fig. 5.** Sensitivity analysis of departure time and comparison between NOMAD and r5r.

glean these insights about the interplay between emerging mobility modes and transit highlights one of NOMAD's strengths relative to other open-source models.

Only during the small time window from 7:50 AM to 7:59 AM does the model indicate that a transit/walking path is optimal. This path requires a transfer between bus lines, and it is the least-cost option only when the transfer is somewhat seamless in terms

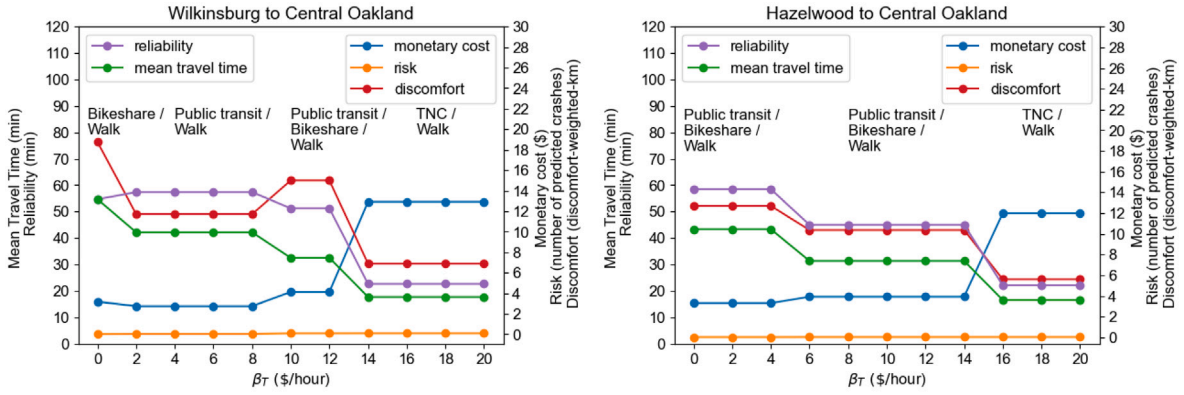


(a) Optimal Path Cost Attributes by $\beta_T$ from Wilkinsburg to Central Oakland.

(b) Optimal Path Cost Attributes by $\beta_T$ from Hazelwood to Central Oakland.

**Fig. 6.** Sensitivity analysis of $\beta_T$.

of waiting time. Results from r5r, depicted in Fig. 5(d), confirm that paths between Hazelwood and Central Oakland always require at least one transfer. Double-transfer routes are not uncommon, which further exposes the limitations of transit coverage for this specific O-D pair. Comparing paths identified by NOMAD and r5r, we observe that NOMAD can determine better feasible options that account for the role of emerging shared modes. We also draw attention to the fact that NOMAD finds transit/walking paths with lower travel times than those found by r5r. This is due to a simplification in our model in the construction of transfer edges. Recall from Section 3.2.2 that the length of a transfer edge between two nodes is estimated as the Haversine distance between the nodes multiplied by a circuity factor. In general, this approximation is reasonable. However, in cases such as the one presented here, this approximate distance may underestimate the true network distance due to geographical constraints. This underestimation, which leads to shorter reported walking times, is represented in this example. Future iterations of the network model could incorporate the true walking network for a more accurate computation of the length of transfer edges and O/D connector edges.

#### 4.3.2. *Case study 2: Sensitivity analysis of $\beta_T$*

The second case study demonstrates how routing analysis is affected by $\beta_T$, the parameter that defines a commuter's value of mean travel time. We varied $\beta_T$ from \$0.00/h to \$20.00/h in increments of \$2.00/h for this study. This range was selected based on a meta-analysis by Li et al. (2010), which aggregated empirical studies on the willingness to pay for travel time savings. Differences in $\beta_T$ reflect differences in demographic group and activity. The remaining $\beta$ parameters were identical to those used in the first experiment, and the analysis was conducted for the 8:15 AM departure time. For each value of $\beta_T$ and O-D pair of interest, we determined the optimal path along with its mode combination and cost attributes. This experiment also served as a model validation step by ensuring that the cost attributes associated with each path mode combination were directionally correct when compared to one another.

First, we analyze the results for the Wilkinsburg origin shown in Fig. 6(a). For commuters with a zero-valued mean travel time, the optimal path modes are bikeshare and walking. The route's monetary cost is expectedly low due to the low use fee for a bikeshare. The longer average travel time is the result of a long initial walking segment to reach a bikeshare station from the origin. For travelers characterized by $\beta_T$ in the range of \$2.00/h to \$8.00/h, the least-cost route changes to transit path with a direct bus line. Though the average travel time declines, the reliability attribute as represented by the 95th percentile travel time increases. This result is expected, since the transit mode is associated with high variation in waiting time whereas the active bikeshare mode is unaffected by traffic conditions per model assumptions. Moreover, the discomfort attribute expectedly decreases due to less physical exertion for a traveler taking the bus relative to a traveler riding a bike. An increase in $\beta_T$ to \$10.00/h and \$12.00/h yields an optimal route characterized by an express bus line for the first segment followed by a bikeshare for the second segment. The mean travel time declines because the express bus has a dedicated lane, passes through fewer stops, and is well-connected to a bikeshare station at the identified transfer point. The predicted number of daily crashes along this route, which is not discernibly different from zero on this graph, more than doubles from 0.041 to 0.096. This change is likely caused by two factors: (1) an express bus that moves on roads with high speed limits, and (2) the inclusion of bikeshare. Once $\beta_T$ reaches \$14.00/h, the path switches to TNC/walking. The estimated monetary cost increases three-to-four-fold relative to the monetary cost of the other path options. Mean travel time, the reliability metric, and the discomfort metric decline as the traveler is taken directly from origin to destination after an initial waiting period. The reduction in these cost attributes thus compensates for the steep rise in price. The crash risk increases by just 3%. From a planning perspective, these results suggest that the high prices of TNC vehicles are justified for traveler groups with high values of travel times, since TNCs are usually quicker, more reliable under light traffic, and more comfortable. Planners aiming to promote transit or active modes in place of TNC may consider investing in micromobility safety infrastructure, new express bus routes, or additional bikeshare stations. These policy suggestions assume that travelers are able-bodied; for users with restrictions, transit agencies may consider partnering with TNC companies for first-/last-mile connections (Uber, 2023).

Second, we examine the effect of $\beta_T$ on the optimal path for this departure time between Hazelwood and Central Oakland, displayed in Fig. 6(b). NOMAD suggests that commuters theoretically desire a transit/bikeshare/walking route for $\beta_T$ in the range of \$0.00/h to \$14.00/h. Interestingly, there are two distinct multimodal paths involving transit, bikeshare, and walking. The first one, which is identified when $\beta_T$ is less than or equal to \$4.00/h, is marked by a longer transit component, a longer walking transfer, and a shorter bikeshare segment. Somewhat surprisingly, the second one involves a shorter transit segment but the outcome corresponds to a lower total travel time. This can be attributed to a shorter walking transfer, where the walking time is replaced by bikeshare use time. The longer bikeshare component of this path also results in a higher monetary cost relative to the other multimodal option. For commuters who value the mean travel time at \$16.00/h, the least-cost path shifts to TNC. Our insights regarding the TNC path are the same as those in the Wilkinsburg case; average travel time, reliability as measured by the 95th percentile, and the discomfort metric all decrease in exchange for a higher monetary cost. The crash risk remains relatively constant, which is sensible according to the mode-specific crash risk indices provided in Table 5. The increased risk of TNC vehicles relative to transit likely compensates for the decreased risk of TNC vehicles relative to bikeshare. Finally, we comment that this experiment was conducted specifically for the 8:15 AM departure time, coinciding with the imminent arrival of a transit vehicle per Fig. 5(b). For other departure times, the shortest path shifts to a TNC/walking at lower values of $\beta_T$.

#### 4.3.3. Case study 3: Sensitivity analysis of scooter usage pricing

In the third case study, we lowered the per-minute use fee of a shared scooter. We tested three prices: \$0.09/min, \$0.19/min, and \$0.29/min. The $\beta$ parameters were identical to those used in the first study. The actual fee of a scooter in Pittsburgh is \$0.39/min, but the previous case studies reveal that free-floating scooters are not a viable mode option at this price point for either O-D pair for travelers with this set of cost sensitivities. The objective of this analysis was to determine if lower-priced scooters have the potential to be a standalone or first-/last-mile mobility solution.

Fig. 7 shows that free-floating scooters can complement other modes if priced low enough. We first examine results for the Wilkinsburg origin. Since Wilkinsburg has robust transit and well-connected bikeshare options, reducing the price to \$0.19/min has no effect on shortest paths relative to Fig. 5(a). This outcome is not surprising; although shared bikes require a fixed pickup/drop-off location, they are more appealing from a monetary perspective since they are priced at \$0.125/min. Furthermore, Table 5 indicates our model's assumption that bikes move faster than scooters. Usage prices must decline to \$0.09/min for shared scooters to become involved in the optimal path for some departure times. At this price, scooter/bikeshare/walking routes replace a few routes that previously involved transit. This is likely because scooter travel times are not prone to day-to-day variation per NOMAD's assumptions, implying a lower reliability cost. The walking travel time to the nearest scooter can certainly vary, though we suspect that the variation turns out to be small as a result of our data generation process that simulated scooter location data.

Fig. 7(b) reveals the benefit of lower scooter prices for the Hazelwood community. The findings align with Fig. 5(b) from the first case study, which exposed this neighborhood's lack of robust transit options. First, we note that decreasing the price to \$0.29/min does not alter the theoretically optimal path. However, when the use fee declines to \$0.19/min, paths that previously included TNCs are replaced by multimodal paths in which a scooter serves as a first-mile solution to bikeshare. The implication is that the lower monetary cost of these paths relative to TNC paths compensates for their longer travel times. In cases of an impending bus arrival, it remains optimal for this traveler group to take a transit route that connects to bikeshare. Only when the price drops to \$0.09/min, which is lower than the use fee of a bikeshare, does NOMAD suggest full scooter paths. These paths have a slightly lower average travel time than scooter/bikeshare/walking paths, even though a scooter's presumed speed is slower than a bike's presumed speed. This difference arises because scooter/bikeshare/walking paths include a transfer, which incurs a transfer penalty cost in the form of travel time. Interestingly, our model never identifies an optimal path using scooter as a first-/last-mile solution to transit for this specific O-D pair. We attribute this result to the relatively high weight of the reliability attribute in the generalized cost function in conjunction with the low reliability of infrequent transit.

Moreover, this analysis shows the model's ability to perform scenario testing. Using the framework, transportation planners can adjust different network elements and determine changes in the optimal path by O-D pair, given a set of otherwise constant model parameters. This case study shows the effects of price reductions, which is relevant for agency and mobility operators who offer discounted rates for low-income groups (Move PGH, 2023). Planners could also conceivably test the effects of a new bikeshare station location or alternate bus routes.

#### 4.3.4. Case study 4: Comparison of accessibility with different modes

The fourth experiment calculates accessibility to jobs for selected origins in the study area under two mode scenarios: transit/walking versus transit/bikeshare/walking. This experiment is more general than the first three, as the results of O-D routing analysis are aggregated to produce a single accessibility metric on the origin-level. Given that accessibility metrics are frequently used in practice to evaluate new policies related to land-use infrastructure (Geurs and van Wee, 2004), this case study highlights a practical use case of NOMAD on a higher level. Its objective is to illustrate the extent to which emerging mobility modes (bikeshare, in this example) can improve accessibility within the study area.

As with prior case studies, origins and destinations are represented by census block group centroids. We used the approach of Wardrip et al. (2015) to determine the number of opportunity occupations in each destination block group, defined as those that pay at least the regional average wage and do not require a bachelor's degree. All opportunity occupations within a destination block group are assumed to be concentrated at the block group's centroid.

We adopted the cumulative opportunities metric of accessibility, which counts a destination's jobs as reachable by an origin if the travel cost between the origin and destination does not exceed some threshold cost value (Curtis and Scheurer, 2010). To

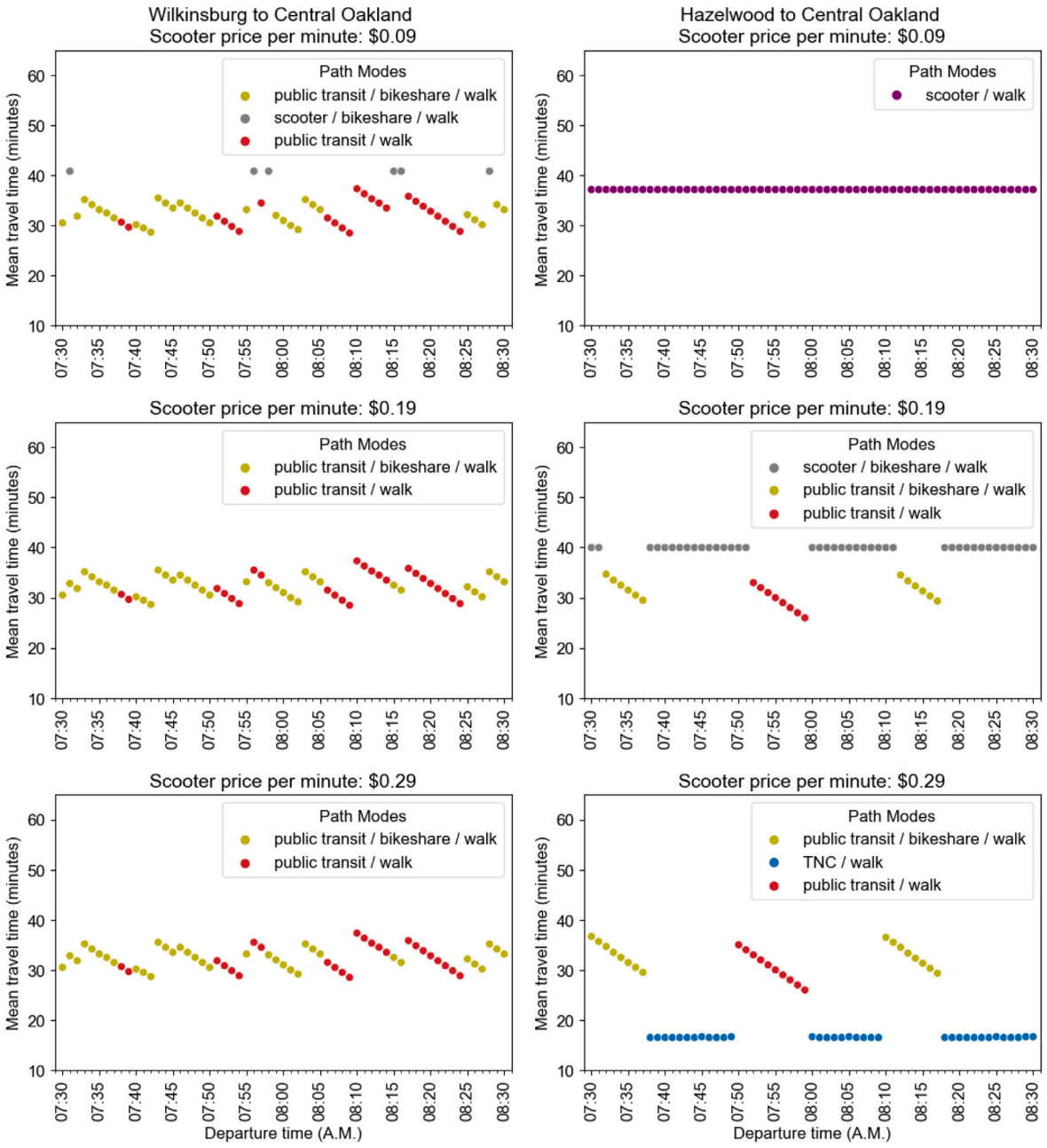


(a) Wilkinsburg to Central Oakland: Effect of Scooter Price Adjustments.

(b) Hazelwood to Central Oakland: Effect of Scooter Price Adjustments.

**Fig. 7.** Sensitivity analysis of scooter pricing.

compute accessibility, we first identified the theoretically optimal path between each O-D pair for each minute from 7:30 AM to 8:00 AM for a single traveler group marked by a set of cost sensitivities. This step required fixing the $\beta$ parameters, and the values from the first and third experiments were selected. Then, the generalized travel cost and cost attributes (mean travel time, reliability as measured by the 95th percentile travel time, monetary cost, crash risk, and discomfort) of the optimal path were extracted. This resulted in a multimodal, multi-cost O-D travel cost matrix keyed by origin, destination, and departure time. Following Conway et al. (2018), we accounted for variation in departure time by selecting the median value of each cost attribute throughout the departure window on the O-D level. The reliability attribute was selected as the travel cost in the cumulative opportunities calculation to showcase an accessibility metric that is more conservative with respect to travel time. The cost threshold was set at 45 minutes. Thus, a destination and its jobs were counted as reachable by an origin if the departure time window's median value of the reliability

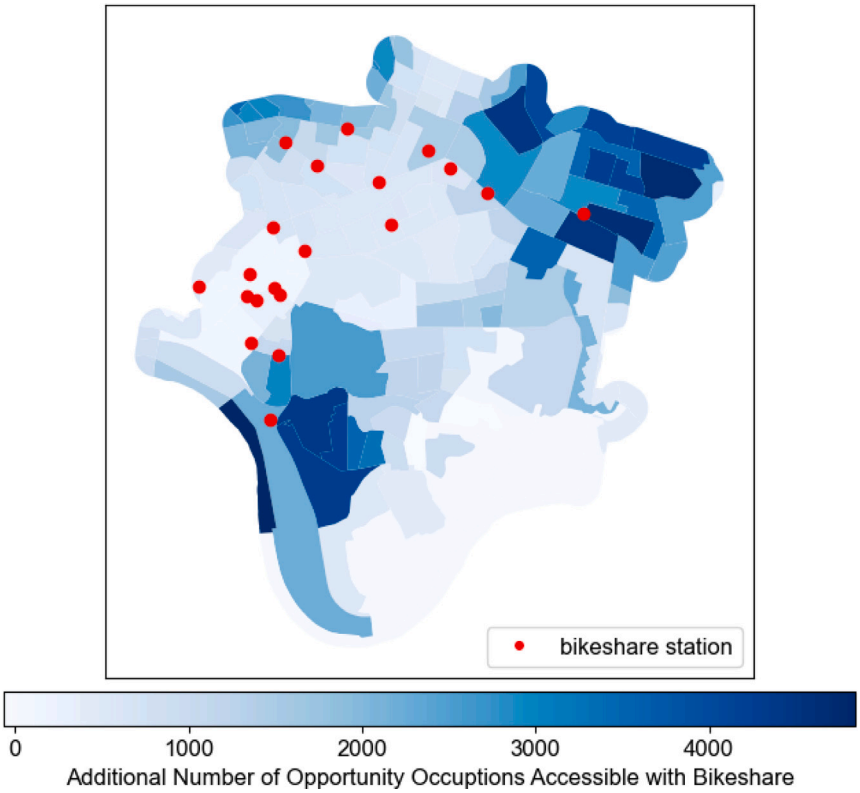


**Fig. 8.** Heatmap of the study area showing the number of additional jobs accessible in the transit/bikeshare/walking mode scenario relative to the transit/walking mode scenario. Bikeshare stations are overlain with red markers.

attribute did not exceed 45 minutes for the O-D pair. This analysis could be readily repeated with other travel cost attributes and cost thresholds.

To evaluate the role of bikeshare as a complement to transit, job accessibility was computed in two cases. In the first case, the supernetwork modes only included public transit and walking. The modes in the second case included public transit, bikeshare, and walking. Fig. 8 displays the number of additional jobs accessible on the origin block group level with the addition of bikeshare. Bikeshare stations are overlain with red markers. This figure suggests that bikeshare can play a significant role in improving accessibility, a result that is consistent with our prior experiments on a smaller scale.

In particular, we observe that origin block groups on the outskirts of the study area experience greater gains despite having fewer bikeshare stations. This result indicates that opportunities for these residents to use bikeshare as a standalone or first-mile solution are limited. However, transit service provides connections to bikeshare so that it may be used as a last-mile solution instead. The fact that job accessibility improves more for origins on the periphery is expected, since residents of these neighborhoods often need to take a transit trip that requires a transfer between bus lines. Paths that involve transfers are unreliable when accounting for the possibility of a missed transfer; hence, these paths are characterized by high 95th percentile travel times. When bikeshare is introduced as a travel mode, the shortest path algorithm instead identifies optimal paths in which bikeshare replaces one of the bus lines. Assuming the availability of bikes at the station, these trips are generally more reliable because commuters are not subject to the uncertain arrival time of a bus. We also observe that origin block groups in the mid-west portion of the study area experience minimal gains in job accessibility despite the prevalence of nearby bikeshare stations. This is because these origins can already reach many jobs through a combination of transit and walking, given that job opportunities are concentrated in this part of the study area. Bikeshare serves as a mode alternative, but transit accessibility for residents of these origins is already relatively high. Finally, we comment that this calculation could be feasibly repeated with a different bikeshare station configuration to quantify the accessibility value of the proposed investment.

## 5. Conclusion

In this paper, we introduced a multimodal, multi-cost, time-dependent network model inclusive of shared emerging mobility options. The model is implemented within NOMAD: Network Optimization for Multimodal Accessibility Decision-making, an open-source tool that can be used to conduct O-D routing analysis and construct multimodal travel cost matrices. These travel cost matrices may serve as an immediate input to accessibility analysis and further inform the formulation of network optimization problems.

This work builds upon previous literature in several ways. First, it establishes a multimodal supernetwork model inclusive of all relevant mobility options: personal vehicle, TNC, carshare, public transit, personal bike, bikeshare, scooter, walking, and feeder micro-transit. Connections among nodes and edges in the supernetwork are designed to allow for any practical transfers between modes. Second, it assigns an edge-based generalized travel cost function that accounts for mean travel time, monetary cost, reliability, crash risk, and discomfort, as well as a node-based cost that can impose additional (dis)incentives for any multimodal trip. Third, it can be tailored to individual groups by controlling the weights of each cost attribute in the edge travel cost function. We can consequently show how optimal paths, generalized travel costs, and mode combinations vary by socio-demographic group. Fourth, it uses a dynamic shortest path algorithm that can output shortest paths for each departure time with a single algorithm run. Conducting time-dependent routing analysis is critical for planners who seek to provide options for travelers during low-frequency transit periods.

We demonstrated the method on a large-scale transportation network in Pittsburgh, PA, which required fusing several data sources. The first experiment explored how the generalized travel cost, average travel time, and mode combination of the theoretically optimal path vary by departure time on the minute-level, confirming that the presence of emerging shared mobility options can complement schedule-based transit both spatially and temporally. In the second case study, we adjusted $\beta_T$, the parameter defining one's value of mean travel time, in the generalized travel cost equation. The results showed how small changes to this parameter influence the shortest path between a specific O-D pair, indicating the importance of considering traveler preferences. This analysis also revealed the generalized travel cost breakdown by cost component and path mode combination, providing planners with more details on the factors that drive shifts in the optimal route. The third case study showed how the framework can be used to test how path options change in conjunction with changes in mode fees. Specifically, we found that scooters can be a viable standalone or first/last-mile solution when they are not prohibitively expensive. The final experiment introduced a cumulative opportunities metric of job accessibility based on the reliability attribute. Accessibility was evaluated under two mode scenarios, and our findings quantified the extent to which bikeshare can improve job accessibility.

In future work, we can calibrate the $\beta$ parameters of the generalized travel cost function using revealed route choices by traveler group. This may be accomplished by applying discrete choice models to survey data or trip-level probe data. We may also obtain historical data for transit performance and scooter locations to more accurately develop the cost function for the relevant edges. In addition, we could include the full walking network if provided with granular sidewalk data. Other applications of the model can be developed for community stakeholders who play a role in the provision of MaaS. These include adjusting prices, availability, and facilities associated with different modes to evaluate expected changes in system-level accessibility. Such an assessment could allow policymakers to optimize decisions on when, where, and how to improve mobility services given accessibility objectives and budget constraints. Another application of special interest is the optimal provision of Universal Basic Mobility programs, which offer community members a fixed monthly credit to be used on shared mobility services.

## CRediT authorship contribution statement

**Lindsay K. Graff:** Writing – review & editing, Writing – original draft, Visualization, Validation, Software, Methodology, Formal analysis, Investigation, Data curation, Conceptualization. **Katherine A. Flanigan:** Writing – review & editing, Supervision, Resources, Methodology, Funding acquisition, Conceptualization. **Sean Qian:** Writing – review & editing, Supervision, Resources, Methodology, Funding acquisition, Conceptualization.

## Declaration of competing interest

The authors declare that they have no known competing financial interests or personal relationships that could have appeared to influence the work reported in this paper.

## Data and code availability

The data used for this work, with the exception of probe vehicle speed data, is publicly available as described in Section Section 4.2. The implementation of NOMAD with experiments is open-source and available at the following link: https://github.com/lgraff/nomad.

## Acknowledgments

This research is supported by *USDOT's National University Transportation Center Mobility21*, United States of America, *the K&L Gates Presidential Fellowship in Ethics and Computational Technologies*, *and in part by National Science Foundation*, United States of America *CMMI-1751448*. The contents of this paper reflect the views of the authors only, who are responsible for the facts and the accuracy of the information presented.

## Data and code availability

The data used for this work, with the exception of probe vehicle speed data, is publicly available as described in Section 4.2. The implementation of NOMAD with experiments is open-source and available at the following link: https://github.com/lgraff/nomad.

## References


Abdelwahab, B., Palm, M., Shalaby, A., Farber, S., 2021. Evaluating the equity implications of ridehailing through a multi-modal accessibility framework. J. Transp. Geogr. 95, 103147. http://dx.doi.org/10.1016/j.jtrangeo.2021.103147.

Alessandretti, L., Natera Orozco, L.G., Saberi, M., Szell, M., Battiston, F., 2023. Multimodal urban mobility and multilayer transport networks. Environ. Plan. B: Urban Anal. City Sci. 50 (8), 2038–2070. http://dx.doi.org/10.1177/23998083221108190, Publisher: SAGE Publications Ltd STM.

Almannaa, M.H., Ashqar, H.I., Elhenawy, M., Masoud, M., Rakotonirainy, A., Rakha, H., 2021. A comparative analysis of e-scooter and e-bike usage patterns: Findings from the City of Austin, TX. Int. J. Sustain. Transp. 15 (7), 571–579. http://dx.doi.org/10.1080/15568318.2020.1833117.

Anderson, P., Owen, A., Levinson, D., 2013. The time between: Continuously defined accessibility functions for schedule-based transportation systems. In: Transportation Research Board 92nd Annual Meeting.

Arbex, R., Cunha, C.B., 2020. Estimating the influence of crowding and travel time variability on accessibility to jobs in a large public transport network using smart card big data. J. Transp. Geogr. 85, 102671. http://dx.doi.org/10.1016/j.jtrangeo.2020.102671.

Beck, L.F., Dellinger, A.M., O'Neil, M.E., 2007. Motor vehicle crash injury rates by mode of travel, United States: Using exposure-based methods to quantify differences. Am. J. Epidemiol. 166 (2), 212–218. http://dx.doi.org/10.1093/aje/kwm064.

Bhat, C.R., 2000. Incorporating observed and unobserved heterogeneity in urban work travel mode choice modeling. Transp. Sci. 34 (2), 228–238. http://dx.doi.org/10.1287/trsc.34.2.228.12306, Publisher: INFORMS.

Braga, C.K.V., Loureiro, C.F.G., Pereira, R.H.M., 2023. Evaluating the impact of public transport travel time inaccuracy and variability on socio-spatial inequalities in accessibility. J. Transp. Geogr. 109, 103590. http://dx.doi.org/10.1016/j.jtrangeo.2023.103590.

Carlier, K., Inro, T., Fiorenzo-Catalano, S., Lindveld, C., Bovy, P., 2002. Supernetwork approach towards multimodal travel modeling. In: Transportation Research Board 82nd Annual Meeting.

Carrion, C., Levinson, D., 2012. Value of travel time reliability: A review of current evidence. Transp. Res. A 46 (4), 720–741. http://dx.doi.org/10.1016/j.tra.2012.01.003, URL: https://www.sciencedirect.com/science/article/pii/S0965856412000043.

Chabini, I., 1998. Discrete dynamic shortest path problems in transportation applications: Complexity and algorithms with optimal run time. Transp. Res. Rec. 1645 (1), 170–175. http://dx.doi.org/10.3141/1645-21.

Chen, J., Ni, J., Xi, C., Li, S., Wang, J., 2017. Determining intra-urban spatial accessibility disparities in multimodal public transport networks. J. Transp. Geogr. 65, 123–133. http://dx.doi.org/10.1016/j.jtrangeo.2017.10.015.

City of Austin, 2022. Austin Strategic Mobility Plan. Technical Report, City of Austin.

City of Boston, 2017. Go Boston 2030. Technical Report, City of Boston.

City Of Pittsburgh, 2022. Move PGH Mid-Pilot Report. Technical Report, Department of Mobility and Infrastructure.

Conveyal, https://docs.conveyal.com/.

Conveyal, 2024b. Conveyal R5 routing engine. https://github.com/conveyal/r5.

Conway, M.W., Byrd, A., Eggermond, M.v., 2018. Accounting for uncertainty and variation in accessibility metrics for public transport sketch planning. J. Transp. Land Use 11 (1).

Conway, M.W., Byrd, A., van der Linden, M., 2017. Evidence-based transit and land use sketch planning using interactive accessibility methods on combined schedule and headway-based networks. Transp. Res. Rec. 2653 (1), 45–53. http://dx.doi.org/10.3141/2653-06, Publisher: SAGE Publications Inc.

Conway, M.W., Stewart, A.F., 2019. Getting Charlie off the MTA: a multiobjective optimization method to account for cost constraints in public transit accessibility metrics. Int. J. Geogr. Inf. Sci. 33 (9).

Cui, M., Levinson, D., 2018. Full cost accessibility. J. Transp. Land Use 11 (1), http://dx.doi.org/10.5198/jtlu.2018.1042, Number: 1.

Curtis, C., Scheurer, J., 2010. Planning for sustainable accessibility: Developing tools to aid discussion and decision-making. Prog. Plan. 74 (2), 53–106. http://dx.doi.org/10.1016/j.progress.2010.05.001.

Dadashova, B., 2022. Addressing Bicyclist safety Through the Development of Crash Modification factors for Bikeways. Technical Report 0-7043-R1, Texas A&M Transportation Institute.

Delling, D., Dibbelt, J., Pajor, T., Wagner, D., Werneck, R.F., 2013. Computing multimodal journeys in practice. In: Bonifaci, V., Demetrescu, C., Marchetti-Spaccamela, A. (Eds.), Experimental Algorithms. Springer, Berlin, Heidelberg, pp. 260–271. http://dx.doi.org/10.1007/978-3-642-38527-8_24.

Delling, D., Pajor, T., Wagner, D., 2009. Accelerating multi-modal route planning by access-nodes. In: Fiat, A., Sanders, P. (Eds.), Algorithms - ESA 2009. Springer, Berlin, Heidelberg, pp. 587–598. http://dx.doi.org/10.1007/978-3-642-04128-0_53.

Delling, D., Pajor, T., Werneck, R.F., 2015. Round-based public transit routing. Transp. Sci. 49 (3), 591–604. http://dx.doi.org/10.1287/trsc.2014.0534.

Dibbelt, J., Pajor, T., Wagner, D., 2015. User-constrained multimodal route planning. ACM J. Exp. Algorithmics 19, 1–19. http://dx.doi.org/10.1145/2699886.

DiGioia, J., Watkins, K.E., Xu, Y., Rodgers, M., Guensler, R., 2017. Safety impacts of bicycle infrastructure: A critical review. J. Saf. Res. 61, 105–119. http://dx.doi.org/10.1016/j.jsr.2017.02.015.

Dimokas, N., Kalogirou, K., Spanidis, P., Kehagias, D., 2018. A Mobile application for multimodal trip planning. In: 2018 9th International Conference on Information, Intelligence, Systems and Applications. IISA, pp. 1–8. http://dx.doi.org/10.1109/IISA.2018.8633665.

Djurhuus, S., Sten Hansen, H., Aadahl, M., Glümer, C., 2016. Building a multimodal network and determining individual accessibility by public transportation. Environ. Plan. B: Plann. Des. 43 (1), 210–227. http://dx.doi.org/10.1177/0265813515602594.

Du, B., Wang, D.Z.W., 2014. Continuum modeling of park-and-ride services considering travel time reliability and heterogeneous commuters – A linear complementarity system approach. Transp. Res. E 71, 58–81. http://dx.doi.org/10.1016/j.tre.2014.08.008.

El-Geneidy, A., Buliung, R., Diab, E., van Lierop, D., Langlois, M., Legrain, A., 2016a. Non-stop equity: Assessing daily intersections between transit accessibility and social disparity across the Greater Toronto and Hamilton Area (GTHA). Environ. Plan. B: Plann. Des. 43 (3), 540–560. http://dx.doi.org/10.1177/0265813515617659.

El-Geneidy, A., Grimsrud, M., Wasfi, R., Tétreault, P., Surprenant-Legault, J., 2014. New evidence on walking distances to transit stops: identifying redundancies and gaps using variable service areas. Transportation 41 (1), 193–210. http://dx.doi.org/10.1007/s11116-013-9508-z.

El-Geneidy, A., Levinson, D., Diab, E., Boisjoly, G., Verbich, D., Loong, C., 2016b. The cost of equity: Assessing transit accessibility and social disparity using total travel cost. Transp. Res. A 91, 302–316. http://dx.doi.org/10.1016/j.tra.2016.07.003.

Fan, Y., Ding, J., Liu, H., Wang, Y., Long, J., 2022. Large-scale multimodal transportation network models and algorithms-Part I: The combined mode split and traffic assignment problem. Transp. Res. E 164, 102832. http://dx.doi.org/10.1016/j.tre.2022.102832.

Farber, S., Fu, L., 2017. Dynamic public transit accessibility using travel time cubes: Comparing the effects of infrastructure (dis)investments over time. Comput. Environ. Urban Syst. 62, 30–40. http://dx.doi.org/10.1016/j.compenvurbsys.2016.10.005.

Foth, N., Manaugh, K., El-Geneidy, A.M., 2013. Towards equitable transit: examining transit accessibility and social need in Toronto, Canada, 1996–2006. J. Transp. Geogr. 29, 1–10. http://dx.doi.org/10.1016/j.jtrangeo.2012.12.008.

Gatersleben, B., Uzzell, D., 2007. Affective appraisals of the daily commute: Comparing perceptions of drivers, cyclists, walkers, and users of public transport. Environ. Behav. 39 (3), 416–431. http://dx.doi.org/10.1177/0013916506294032.

Gehrke, S.R., Akhavan, A., Furth, P.G., Wang, Q., Reardon, T.G., 2020. A cycling-focused accessibility tool to support regional bike network connectivity. Transp. Res. D 85, 102388. http://dx.doi.org/10.1016/j.trd.2020.102388.

Geurs, K.T., van Wee, B., 2004. Accessibility evaluation of land-use and transport strategies: review and research directions. J. Transp. Geogr. 12 (2), 127–140. http://dx.doi.org/10.1016/j.jtrangeo.2003.10.005.
Giacomin, D.J., Levinson, D.M., 2015. Road network circuity in metropolitan areas. Environ. Plan. B: Plann. Des. 42 (6), 1040–1053. http://dx.doi.org/10.1068/b130131p.
GraphHopper, https://www.graphhopper.com/.
Guzman, L.A., Oviedo, D., Rivera, C., 2017. Assessing equity in transport accessibility to work and study: The Bogotá region. J. Transp. Geogr. 58, 236–246. http://dx.doi.org/10.1016/j.jtrangeo.2016.12.016.
Hrnčíř, J., Jakob, M., 2013. Generalised time-dependent graphs for fully multimodal journey planning. In: 16th International IEEE Conference on Intelligent Transportation Systems (ITSC 2013). pp. 2138–2145. http://dx.doi.org/10.1109/ITSC.2013.6728545.
Huang, H., Bucher, D., Kissling, J., Weibel, R., Raubal, M., 2019. Multimodal route planning with public transport and carpooling. IEEE Transactions on Intelligent Transportation Systems 20 (9), 3513–3525. http://dx.doi.org/10.1109/TITS.2018.2876570.
Jensen, P., Rouquier, J.-B., Ovtracht, N., Robardet, C., 2010. Characterizing the speed and paths of shared bicycle use in Lyon. Transp. Res. D 15 (8), 522–524. http://dx.doi.org/10.1016/j.trd.2010.07.002.
Kar, A., Le, H.T.K., Miller, H.J., 2023. Inclusive accessibility: Integrating heterogeneous user mobility perceptions into space-time prisms. Ann. Am. Assoc. Geogr. 113 (10), 2456–2479. http://dx.doi.org/10.1080/24694452.2023.2236184.
Kelobonye, K., McCarney, G., Xia, J.C., Swapan, M.S.H., Mao, F., Zhou, H., 2019. Relative accessibility analysis for key land uses: A spatial equity perspective. J. Transp. Geogr. 75, 82–93. http://dx.doi.org/10.1016/j.jtrangeo.2019.01.015.
Levinson, D., King, D., 2020. Transport Access Manual: A Guide for Measuring Connection Between People and Places. Committee of the Transport Access Manual, University of Sydney, URL: https://ses.library.usyd.edu.au/handle/2123/23733.
Li, Z., Hensher, D.A., Rose, J.M., 2010. Willingness to pay for travel time reliability in passenger transport: A review and some new empirical evidence. Transp. Res. E 46 (3), 384–403. http://dx.doi.org/10.1016/j.tre.2009.12.005.
Li, X., Luo, Y., Wang, T., Jia, P., Kuang, H., 2020. An integrated approach for optimizing bi-modal transit networks fed by shared bikes. Transp. Res. E 141, 102016. http://dx.doi.org/10.1016/j.tre.2020.102016.
Liao, F., Arentze, T., Timmermans, H., 2010. Supernetwork approach for multimodal and multiactivity travel planning. Transp. Res. Rec. 2175 (1), 38–46. http://dx.doi.org/10.3141/2175-05.
Liezenga, A.M., Verma, T., Mayaud, J.R., Aydin, N.Y., van Wee, B., 2024. The first mile towards access equity: Is on-demand microtransit a valuable addition to the transportation mix in suburban communities? Transp. Res. Interdiscip. Perspect. 24, 101071. http://dx.doi.org/10.1016/j.trip.2024.101071.
Liu, L., 2010. Data Model and Algorithms for Multimodal Route Planning with Transportation Networks (Doctoral dissertation). Technical University of Munich.
Liu, Y., Lyu, C., Liu, Z., Cao, J., 2021. Exploring a large-scale multi-modal transportation recommendation system. Transp. Res. C 126, 103070. http://dx.doi.org/10.1016/j.trc.2021.103070.
Liu, L., Miller, H.J., 2022. Measuring the impacts of dockless micro-mobility services on public transit accessibility. Comput. Environ. Urban Syst. 98, 101885. http://dx.doi.org/10.1016/j.compenvurbsys.2022.101885.
Liu, L., Porr, A., Miller, H.J., 2023. Realizable accessibility: evaluating the reliability of public transit accessibility using high-resolution real-time data. J. Geogr. Syst. 25 (3), 429–451. http://dx.doi.org/10.1007/s10109-022-00382-w.
Ma, W., Pi, X., Qian, S., 2020. Estimating multi-class dynamic origin-destination demand through a forward-backward algorithm on computational graphs. Transp. Res. C 119, 102747.
Ma, W., Xidong, P., Zou, Q., Qian, S., 2024. MAC-POSTS. https://github.com/maccmu/macposts.
Maria, E., Budiman, E., Haviluddin, Taruk, M., 2020. Measure distance locating nearest public facilities using Haversine and Euclidean methods. J. Phys. Conf. Ser. 1450 (1), 012080. http://dx.doi.org/10.1088/1742-6596/1450/1/012080.
Mavoa, S., Witten, K., McCreanor, T., O'Sullivan, D., 2012. GIS based destination accessibility via public transit and walking in Auckland, New Zealand. J. Transp. Geogr. 20 (1), 15–22. http://dx.doi.org/10.1016/j.jtrangeo.2011.10.001.
McCrum, C., Willems, P., Karamanidis, K., Meijer, K., 2019. Stability-normalised walking speed: A new approach for human gait perturbation research. J. Biomech. 87, 48–53. http://dx.doi.org/10.1016/j.jbiomech.2019.02.016.
Move PGH, 2023. Affordable mobility is for everyone. https://move-pgh.com/affordable.
Moya-Gómez, B., García-Palomares, J.C., 2017. The impacts of congestion on automobile accessibility. What happens in large European cities? J. Transp. Geogr. 62, 148–159. http://dx.doi.org/10.1016/j.jtrangeo.2017.05.014.
Ni, P., Vo, H.T., Dahlmeier, D., Cai, W., Ivanchev, J., Aydt, H., 2015. DEPART: Dynamic route planning in stochastic time-dependent public transit networks. In: 2015 IEEE 18th International Conference on Intelligent Transportation Systems. (ISSN: 2153-0017) pp. 1672–1677. http://dx.doi.org/10.1109/ITSC.2015.271.
O*NET Resource Center, 2024. Education, training, and experience.
OpenTripPlanner, https://www.opentripplanner.org/.
OpenTripPlanner, https://github.com/opentripplanner/OpenTripPlanner.
Owen, A., Levinson, D.M., 2015. Modeling the commute mode share of transit using continuous accessibility to jobs. Transp. Res. A 74, 110–122. http://dx.doi.org/10.1016/j.tra.2015.02.002.
Pereira, R.H.M., Herszenhut, D., Saraiva, M., Farber, S., 2024a. Ride-hailing and transit accessibility considering the trade-off between time and money. Cities 144, 104663. http://dx.doi.org/10.1016/j.cities.2023.104663.
Pereira, R.H.M., Saraiva, M., Herszenhut, D., Braga, C.K.V., Conway, M.W., 2021. R5r: Rapid realistic routing on multimodal transport networks with $r^5$ in R. Findings http://dx.doi.org/10.32866/001c.21262, Publisher: Findings Press.
Pereira, R.H.M., Saraiva, M., Herszenhut, D., Braga, C.K.V., Conway, M.W., Luyu, L., 2024b. R5r package source code. https://rdrr.io/cran/r5r/src/R/assign.R.
Pereira, R.H.M., Saraiva, M., Herszenhut, D., Braga, C.K.V., Conway, M.W., Luyu, L., 2024c. R5r: Rapid realistic routing with 'R5'. R package version 2.0. https://cran.r-project.org/web/packages/r5r/r5r.pdf.
Pritchard, J.P., Tomasiello, D.B., Giannotti, M., Geurs, K., 2019. Potential impacts of bike-and-ride on job accessibility and spatial equity in São Paulo, Brazil. Transp. Res. A 121, 386–400. http://dx.doi.org/10.1016/j.tra.2019.01.022.
Pu, W., 2011. Analytic relationships between travel time reliability measures. Transp. Res. Rec. 2254 (1), 122–130. http://dx.doi.org/10.3141/2254-13.
Pyrga, E., Schulz, F., Wagner, D., Zaroliagis, C., 2008. Efficient models for timetable information in public transportation systems. ACM J. Exp. Algorithmics 12, 1–39. http://dx.doi.org/10.1145/1227161.1227166.
Qian, X., Niemeier, D., 2019. High impact prioritization of bikeshare program investment to improve disadvantaged communities' access to jobs and essential services. J. Transp. Geogr. 76, 52–70. http://dx.doi.org/10.1016/j.jtrangeo.2019.02.008, URL: https://www.sciencedirect.com/science/article/pii/S0966692318305374.
Quarmby, D.A., 1967. Choice of travel mode for the journey to work: Some findings. J. Transp. Econ. Policy 1 (3), 273–314.
Saraiva, M., Barros, J., 2022. Accessibility in São Paulo: An individual road to equity? Appl. Geogr. 144, 102731. http://dx.doi.org/10.1016/j.apgeog.2022.102731.
Stępniak, M., Pritchard, J.P., Geurs, K.T., Goliszek, S., 2019. The impact of temporal resolution on public transport accessibility measurement: Review and case study in Poland. J. Transp. Geogr. 75, 8–24. http://dx.doi.org/10.1016/j.jtrangeo.2019.01.007.
Susilo, Y.O., Cats, O., 2014. Exploring key determinants of travel satisfaction for multi-modal trips by different traveler groups. Transp. Res. A 67, 366–380. http://dx.doi.org/10.1016/j.tra.2014.08.002.

Tahmasbi, B., Mansourianfar, M.H., Haghshenas, H., Kim, I., 2019. Multimodal accessibility-based equity assessment of urban public facilities distribution. Sustainable Cities Soc. 49, 101633. http://dx.doi.org/10.1016/j.scs.2019.101633.

Uber, 2023. Case study: DART goes big in 30 zones. https://www.uber.com/blog/case-study-dart-goes-big-in-30-zones/.

U.S. Bureau of Labor Statistics, 2022. Employment projections.

U.S. Census Bureau, 2020. LEHD origin-destination employment statistics.

U.S. Census Bureau, 2022. Selected economic characteristics, 2018–2022 American community survey 5-year estimates.

Valhalla, https://github.com/valhalla/valhalla.

Vredin Johansson, M., Heldt, T., Johansson, P., 2006. The effects of attitudes and personality traits on mode choice. Transp. Res. A 40 (6), 507–525. http://dx.doi.org/10.1016/j.tra.2005.09.001.

Wang, M., Mu, L., 2018. Spatial disparities of Uber accessibility: An exploratory analysis in Atlanta, USA. Comput. Environ. Urban Syst. 67, 169–175. http://dx.doi.org/10.1016/j.compenvurbsys.2017.09.003.

Wardrip, K., Fee, K.D., Nelson, L.A., Andreason, S., 2015. Identifying Opportunity Occupations in the Nation's Largest Metropolitan Economies. Technical Report, Federal Reserve Banks.

Western Pennsylvania Regional Data Center, http://www.wprdc.org/.

Yang, Y., Zhang, W., Lin, H., Liu, Y., Qu, X., 2024. Applying masked language model for transport mode choice behavior prediction. Transp. Res. A 184, 104074. http://dx.doi.org/10.1016/j.tra.2024.104074.

Ye, J., Jiang, Y., Chen, J., Liu, Z., Guo, R., 2021. Joint optimisation of transfer location and capacity for a capacitated multimodal transport network with elastic demand: a bi-level programming model and paradoxes. Transp. Res. E 156, 102540. http://dx.doi.org/10.1016/j.tre.2021.102540.

Zhang, J., Liao, F., Arentze, T., Timmermans, H., 2011. A multimodal transport network model for advanced traveler information systems. Procedia - Soc. Behav. Sci. 20, 313–322. http://dx.doi.org/10.1016/j.sbspro.2011.08.037.

Zheng, Y., Li, W., Qiu, F., Wei, H., 2019. The benefits of introducing meeting points into flex-route transit services. Transp. Res. C 106, 98–112. http://dx.doi.org/10.1016/j.trc.2019.07.012.